Journal of the Geological Society

End of the Kiaman Superchron in the Permian of SW England: Magnetostratigraphy of the Aylesbeare Mudstone and Exeter groups.

--Manuscript Draft--

Manuscript Number:	jgs2015-141
Article Type:	Research article
Full Title:	End of the Kiaman Superchron in the Permian of SW England: Magnetostratigraphy of the Aylesbeare Mudstone and Exeter groups.
Short Title:	Magnetostratigraphy of the Permian of SW England
Corresponding Author:	Mark William Hounslow, phd Lancaster University
Corresponding Author E-Mail:	m.hounslow@lancs.ac.uk
Other Authors:	Gregg McIntosh
	Richard Andrew Edwards
	Deryck J.C Laming
	Vassil Karloukovski
Abstract:	Chronology of Permian strata in SW England is fragmentary and largely based on radiometric dating of associated volcanic units. Magnetostratigraphy from the ~2 km of sediments from in the Exeter and Aylesbeare Mudstone groups was undertaken to define a detailed chronology, using the end of the Kiaman superchron, and the overlying reverse and normal polarity in the Middle and Upper Permian as age constraints. The palaeomagnetic directions are consistent with other European Permian palaeopoles;, with data passing fold and reversal tests. The end of the Kiaman superchron (in the Wordian) occurs in the uppermost part of the Exeter Group. The overlying Aylesbeare Mudstone Group is early Capitanian to latest Wuchiapingian in age. The Changhsingian and most of the Lower Triassic is absent. Magnetostratigraphic comparison with the Southern Permian Basin shows that the Exeter and Aylesbeare Mudstone groups are closely comparable in age to the Havel and Elbe Subgroups of the Rotleigend II succession. The Altmark unconformities in these successions appear similar in age as the sequence boundaries in SW England, indicating both may be climate controlled. Clasts in the Exeter Group, from unroofing of the Dartmoor granite, first occurred at a minimum of ~8 Ma after formation of the granite.
Manuscript Classifications:	Dating (radiometric, absolute, etc); Palaeomagnetism; Stratigraphy
Additional Information:	
Question	**Response**
Are there any conflicting interests, financial or otherwise?	No
Samples used for data or illustrations in this article have been collected in a responsible manner	Confirmed

End of the Kiaman Superchron in the Permian of SW England: Magnetostratigraphy of the Aylesbeare Mudstone and Exeter groups.

Mark W. Hounslow*[1], Gregg McIntosh[2], Richard A. Edwards[3], Deryck J.C. Laming[4], Vassil Karloukovski[1]

[1]*Lancaster Environment Centre, Lancaster University, Lancaster, LA1 4YW, U.K.*
[2] *School of Human and Life Science, Canterbury Christchurch University, Canterbury, UK.*
[3]*Hawkridge, Thorverton, Devon, EX5 5JL, U.K (formerly British Geological Survey, Exeter, UK)*
[4]*Herrington Geoscience and David Roche GeoConsulting, Renslade House, Bonhay Road, Exeter EX4 3AY, Devon, UK.*

*Corresponding author (e-mail: m.hounslow@lancaster.ac.uk :Tel:+ 44 (0) 1524 510238

Abstract: Chronology of Permian strata in SW England is fragmentary and largely based on radiometric dating of associated volcanic units. Magnetostratigraphy from the ~2 km of sediments in the Exeter and Aylesbeare Mudstone groups was undertaken to define a detailed chronology, using the end of the Kiaman superchron, and the overlying reverse and normal polarity in the Middle and Upper Permian as age constraints. The palaeomagnetic directions are consistent with other European Permian palaeopoles; with data passing fold and reversal tests. The end of the Kiaman superchron (in the Wordian) occurs in the uppermost part of the Exeter Group. The overlying Aylesbeare Mudstone Group is early Capitanian to latest Wuchiapingian in age. The Changhsingian and most of the Lower Triassic is absent. Magnetostratigraphic comparison with the Southern Permian Basin shows that the Exeter and Aylesbeare Mudstone groups are closely comparable in age to the Havel and Elbe Subgroups of the Rotleigend II succession. The Altmark unconformities in these successions appear similar in age as the sequence boundaries in SW England, indicating both may be climate controlled. Clasts in the Exeter Group, from unroofing of the Dartmoor granite, first occurred at a minimum of ~8 Ma after formation of the granite.

Supplementary material: Additional magnetic fabric and palaeomagnetic data is available at: hhttp://www.geolsoc.org.uk/SUP000

Permian-Triassic successions in southern and SW England were generated following the Variscan orogeny and occur in a number of interconnected, sag and fault-bounded basins, the largest being the Wessex Basin, and various sub-basins that form the Channel Approaches Basin. Some contain upto 8 km of post-Variscan red-bed fill (Harvey *et al.* 1994; Hamblin *et al*. 1992; Butler 1998; McKie & Williams 2009; Fig. 1). The Wessex Basin formed on Rheno-Hercynian basement (Variscan), between the Northern Variscan Front and the Lizard-Rhenish Suture. The sub-basins of the Western Approaches Basin formed on Saxo-Thuringian (Variscan) and Rheno-Hercynian basement (McCann *et al*. 2006; Strachan *et al.* 2014). As such, these basins may share similar tectonic and stratigraphic histories with similarly situated basins in France and Germany such the Saar-Nahe and Saale basins in Germany (Roscher & Schneider 2006; McCann *et al*. 2006.). However, the tectono-stratigraphic understanding of the UK basins are poorly integrated into the framework of Permian European basin evolution. These intramontane basins often lack the distinctive late Permian carbonate-evaporite, Zechstein successions, common in basins (e.g. Southern Permian Basin) north of the Variscan front, and lack the early Permian faunas of the southern Variscan basins (Roscher & Schneider 2006; McCann *et al*. 2006).

The onshore Permian-Triassic successions in the western parts of the Wessex Basin and the Credition Trough outcrop as the Exeter, Aylesbeare Mudstone and Sherwood Sandstone groups (Figs. 1 & 2). The coastal outcrops form part of the Jurassic Coast World Heritage Site (Barton *et al.* 2011). The work of the British Geological Survey, related to the re-mapping of the Exeter area (Edwards *et al*. 1997), generated a better regional understanding of the Exeter Group (Grp) that was dated to the Permian. The oldest successions outcrop in the Crediton Trough (and Torbay area) may extend into the latest Carboniferous (Edwards *et al*. 1997; Leveridge *et al*. 2003). The units below the base of the Whipton Formation (Fm) in the Exeter and Crediton Trough area contain a variety of basaltic and lamprophyric lavas and intrusions whose Ar-Ar and K-Ar ages (291-282 Ma) are older than the more tightly constrained Rb-Sr, U-Pb and Ar-Ar ages (at 280 Ma) of the formation of the Dartmoor Granite (Scrivener 2006). These volcanic and igneous units are coeval with widespread volcanic activity throughout Europe during the latest Carboniferous to early Permian (Timmerman 2004). The isostatic uplift and regional denudation coeval with and following the granite emplacement, was probably responsible for a major unconformity (Edwards *et al*. 1997) separating the Whipton Fm from the older units (Fig. 2).

Miospores from the Whipton Fm around Exeter, and younger units equivalent to the Alphington and Heavitree Breccia formations demonstrate similarities to assemblages from the Russian Kazanian and Tatarian regional stages (Warrington & Scrivener 1990; Edwards *et al*. 1999). Consequently, the barren overlying Aylesbeare Mudstone Grp has been placed into the Lower Triassic in some subsequent studies (Newell 2001; Benton *et al*. 2002). Since the Aylesbeare Mudstone Grp is widespread in the Wessex Basin and the western approaches (Hamblin *et al.* 1992; Butler 1998; Evans 1990; Barton *et al.* 2011), a Lower Triassic mudstone-dominated lacustrine unit creates a major palaeogeographic problem. That is, southerly-derived clasts in the Lower Triassic units, in central and Northern Britain, could not have been sourced through the Wessex Basin, from the Armorican supply areas to the south, as has been widely concluded for over 100 years (Ussher 1876; Thomas 1909; Wills 1970; McKie & Williams 2009; Morton *et al.* 2013).

To resolve this problem, and constrain in detail the age of the Permian successions we use magnetostratigraphy as a dating tool. The Kiaman (reverse polarity) superchron (KRPS) extends from the mid Carboniferous to the mid Permian, but had ended by the early Wordian (mid Guadalupian), after which reverse and normal polarity intervals (here called the Illawarra superchron) occur during the remainder of the mid and late Permian, extending into the Triassic (Steiner 2006; Hounslow submitted). We demonstrate the stratigraphic position of the end of the KRPS, and the polarity pattern through the upper part of these successions, below the Budleigh Salterton Pebble Beds Fm. This new data allows a much better understanding of age in these units, and their relationship to the much better studied successions in the Southern Permian Basin.

Geology and Lithostratigraphy

Excellent exposures of the Exeter Grp occur in a series of cliff and foreshore exposures between Torbay and Exmouth. The successions are predominantly the deposits of a number of alluvial fans, with aeolian dune sandstones dominating in the Dawlish Sandstone Fm, and also in some units in the Torbay Breccia Fm (Fig. 2). The coastal successions in Torbay are separated from those north of Oddicombe (Fig. 1), by the Torquay-Babbacombe promontory which was a palaeogeographic feature in the Permian (Laming, 1966). Mapping work (by DJCL) indicates the Torbay Breccia Fm (Leveridge *et al*. 2003), can be divided into a number of separate breccias units with differing clast content (Laming & Buller, in prep). The Watcombe Fm which is an onlapping mudstone-rich breccia unit, which is unconformably overlain by the Oddicombe Breccia Fm north of the Torquay-Babbacombe promontory, and the equivalent Paignton breccias in Torbay. On the coastal outcrops the Watcombe Fm has a 9-20^o dip-discordance with the overlying Oddicombe Breccia (9^o at Whitsand Bay and 20^o Oddicombe Cove; Figs. 1, 3; Laming 1982). The lower parts of the Torbay Breccia Fm (Roundham Head breccias, with clasts derived from SW) are generally poor in volcanic clasts (Laming 1982) like the oldest unit (the Cadbury Breccia Fm; Edwards *et al*. 1999) in the Crediton Trough, and by inference may have similar ages, prior to the major early Permian volcanism.

The various breccia units below the Dawlish Sandstone Fm are largely distinguished on their clast contents, which contain a variety of lithologies (limestone, sandstone, vein quartz, quartzite and slate) from various Variscan basement units, together with a variety of volcanic rock fragments associated with the granite and its former or earlier extrusives (Laming 1982; Selwood *et al*. 1984; Edwards & Scrivener 1999). The Watcombe and Whipton formations consist of fine-grained sandy or muddy breccia with clasts of slate and sandstone with occasional porphyry. They contain irregularly interbedded sandstone and mudstone units (Ussher 1913), which dominate the Whipton Fm around Exeter (Edwards & Scrivener 1999). The Oddicombe Breccia Fm (Fig. 2) is rich in locally derived limestone fragments, which typically displays fining-up sequences (into poorly sorted sandstones or fine-breccias; Benton *et al*. 2002) several metres thick, well displayed at Maidencombe Cove and Bundle Head (Fig. 4). The Alphington Breccia Fm is likewise rich in locally derived shale and sandstone fragments, and hornfelised shale from the underlying Variscan basement (Edwards *et al*. 1997). The Teignmouth and Heavitree formations are distinctive for the common presence of clasts of pink and white perthitic feldspar (murchisonite), which Dangerfield & Hawkes (1969) interpreted as feldspar megacrysts from the roof zone of the Dartmoor granite; the supply of which, probably indicates synchronous unroofing into adjacent alluvial fan successions. The Alphington and Oddicombe Breccia formations lack the murchisonite clasts (Selwood *et al*. 1984; Edwards & Scrivener 1999).

All the breccia units tend to be poorly sorted, and may locally contain a high proportion of mud or sand. The fining-up successions in the Teignmouth Breccia Fm, tend to be smaller scale (< 1 m), and typically display poor lateral organisation. Breccias in the upper-parts of this formation have interbedded aeolian sandstone units, well displayed in the Coryton Cove area (8 on Fig. 1; Fig. 4); which is a transitional part of this formation into the overlying Dawlish Sandstone Fm.

The estimated thicknesses of the Oddicombe and Teignmouth Breccia formations vary widely between different authors, because of faulting, variable bedding dips and probably significant palaeotopography on the Variscan basement. The thicknesses of Selwood *et al.* (1984) are minimum thickness estimates, whereas Laming (1969; 1982) and this work suggest greater thicknesses at the upper limits indicated in Fig. 2.

The aeolian dunes systems that dominate deposition in the Dawlish Sandstone Fm (Newell 2001), also display interbedded alluvial sandstone and breccia units. Around Exeter and further north in the Crediton Trough, this formation onlaps onto older units, to rest on Variscan basement. The Exe Breccia Fm is divisible into a lower porphyry-bearing unit (the Kenton Mbr), typical of most of the outcrop on the west of the Exe Estuary, and an overlying quartzite- and mudstone-bearing breccia (the Langstone Mbr). This upper member is well exposed at Langstone Rock (6 on Fig. 1) which in the upper part is dominated by poorly sorted sandstones and sandy siltstones (Gallois 2014; Fig. 4). The thickness of the Exe Breccia is uncertain, due to faulting along the Exe Estuary; 85 m was suggested by Selwood *et al.* (1984), but upto ~50 m is more likely (Laming & Roche 2013) . The uppermost part of the Langstone Mbr at Lympstone and Sowden Lane (3 on Fig. 1) displays both well-developed shallow fluvial channels and aeolian sandstone units, and is gradational into the mudstones and siltstones forming the base of the Aylesbeare Mudstone Grp (Gallois 2014; Fig. 4). Around Exeter and in the Crediton Trough the Aylesbeare Mudstone Grp is unconformable on the Dawlish Sandstone Fm, onlapping onto older units (Edwards *et al.* 1997; Edwards & Scrivener 1999).

Aylesbeare Mudstone Group

The Exmouth Mudstone and Sandstone Fm is a lacustrine, red-brown mudstone-dominated unit with interbedded fine to medium-grained fluvial and lacustrine sandstone units (thicker beds labelled as Beds A to J by Selwood *et al.* 1984). These are most prominent towards the upper part of the formation, where the term Straight Point Sandstone Member is introduced for these persistent sandstone beds (i.e. beds I and J of Selwood *et al.* 1984) which are mapped between the coast and Aylesbeare, north of which the Aylesbeare Mudstone Grp is not sub-divided (Edwards & Scrivener 1999). The upper few metres of the Straight Point Sandstone Mbr at outcrop has patchily developed immature nodular and sheet-like groundwater calcretes, locally with rhizoconcretions (Fig. 3B). The base of the overlying Littleham Mudstone Fm is taken at the base of the porphyry and murchisonite bearing breccia unit (Ormerod-Wareing, 1875), which locally erosively overlies this calcrete-bearing sandstone (Fig. 3C), and grades into overlying interbedded sandstone, siltstone and mudstone beds in the basal parts of the Littleham Mudstone Fm west of the Littleham Cove fault (Fig. 5).

The Littleham Mudstone Fm is well-exposed in the cliffs between Littleham Cove and Budleigh Salterton, but is locally disrupted by faulting in the lower part and slumping in the cliff. The complete succession in the cliffs was determined by using a montage of photographs taken from offshore, which allow the full succession to be divided by a number of prominent green mudstone, thin sandstone and siltstone beds (Fig. 5). The succession in the cliffs can be divided into three units, a lower unit (Division A) east of the Littleham Cove fault with a few green mudstone beds, a middle unit (Division B) with relatively common sandstone and siltstone beds, and an upper unit (Division C) with more frequent green mudstone beds and some impersistant sandstones. The true thickness of the Littleham Mudstone Fm, in these outcrops, cannot be determined because of the uncertain displacement on the Littleham Cove fault. However, the measured cumulative thickness east and west of the fault (216 m), is similar to the ~205 m and 230 m measured in the Blackhill and Withycombe Rayleigh boreholes respectively (Bateson & Johnson 1992; Fig. 1), so the cliff outcrops probably represent most of the Littleham Mudstone Fm. In the Venn Ottery borehole (Fig. 1) the Littleham Mudstone Fm contains pods and veins of gypsum, and thin interbedded aeolian sandstones (Bateson & Johnson 1992; Edwards & Scrivener 1999; N.S Jones pers comm to RAE). A substantial unconformity separates the Littleham Mudstone Fm from the overlying Budleigh Salterton Pebble Beds Fm, shown by the dramatic lithology change, the sharp and irregular boundary (Fig. 3A) with some authors suggesting a small bedding dip difference (Irving, 1888). Gallois (2014) has suggested this contact is conformable.

Regional relationships

Broadly the Permian units in the study area can be divided into 5 genetic sequences (Pm1 to Pm5), bounded by hiatus or unconformity (Fig. 2). The upper three of these are all characterised by basal breccias units (low stand deposits), with conformable transitions into with finer-grained upper parts. The relationships of the successions in Torbay, to those in the Crediton Trough, area is less certain. It is probable that the earliest parts of the Torbay Breccia Fm is timing-related to the Cadbury Breccia Fm in the Crediton Trough (sequence Pm1), since both units are very poor in igneous clasts (Edwards *et al.* 1997). These five sequences may relate to the four sequences seen in the Plymouth Bay Basin (Harvey *et al.* 1994). Their oldest megasequence A, likely relates to Pm1, and megasequence B to Pm2, since it is capped by an inferred volcanic unit. Megasequence C likely relates to Pm3, and is marked by a change in orientation of the Plymouth Bay Basin depocentres. Divergent bedding dips between units under and overlying the Watcombe Fm (Pm2), suggest that the most important extensional event (Leveridge *et al*. 2003; Laming 1982) is at the Pm2-Pm3 boundary, consistent with the basin orientation change. Megasequence D is probably equivalent to Pm4 and Pm5, since the Pm4-Pm5 boundary is subtle to detect in the field.

The continuity of these units to the east in the central parts of the Wessex Basin is uncertain. Henson (1972) suggested, based on geophysics, that the breccia units thin to the east, so eastwards the breccias may pass into the mudstone dominated units, equated with the Aylesbeare Mudstone Grp in the central parts of the Wessex Basin, which are up to ~1.5 km thick (Butler 1998; Hamblin *et al*. 1992). However, Henson's data failed to detect the faults, along the Exe Estuary, so the interpretation may be flawed. In the Western Approaches basins 1 km or more of anhydritic mudstones and sandstones underlie the equivalent of the Sherwood Sandstone Grp (Evans 1990). These locally rest on a Permian volcanic sequence, presumably of a similar age to the early Permian Exeter Volcanic Rocks (Chapman 1989).

Palaeomagnetic sampling

Almost the entire succession of the Aylesbeare Mudstone Grp is exposed in the sea-cliffs between Budleigh Salterton and Exmouth. Only the mid and upper parts of the Exe Breccia could be sampled at Lympstone (3 on Fig.1) and Langstone Rock (6 on Fig. 1; see Supplementary data for details). Outcrops in the lower parts of the Exe Breccia Fm (Kenton Mbr), where all too coarse-grained for palaeomagnetic sampling. Most of the Dawlish Sandstone and Teignmouth Breccia are well exposed between Langstone Rock and Teignmouth, adjacent to the main London-Penzance railway-line (Ussher 1913; Selwood *et al.* 1984), but large parts are inaccessible due to rail-safety restrictions. The Dawlish Sandstone Fm was sampled in quarries near Exeter (4 and 5 on Fig. 1; Fig. 4). The uppermost part of the Teignmouth Breccia was available for sampling in the Coryton Cove and Dawlish Station sections (7 and 8 on Figs. 1,4). Reconnaissance sampling of the Oddicombe and Watcombe Breccias was undertaken. For the most part, these units are fully exposed in sea-cliffs and foreshore exposes between Teignmouth and Oddicombe (Fig. 4). The Knowle Sandstone Fm was sampled at west Sandford (Edwards *et al.* 1997).

Samples from these units were collected using mostly hand samples, oriented with a compass. In total some 153 samples were collected from 13 sites (see Supplementary data), largely focussed on reddened lithologies. Cubic specimens were cut from the hand samples using a circular saw. Some samples from sandstone units in the Dawlish Sandstone and Exe and Teignmouth Breccias were poorly consolidated, and were impregnated with a 2:1 mix of sodium silicate and water (Kostadinova *et al*. 2004) to consolidate them prior specimen preparation.

Laboratory Methodology

Measurements of Natural Remanent Magnetisation (NRM) were made using a CCL 3-axis cryogenic magnetometer (noise level ~0.002 mA/m), using multiple specimen positions, from which the magnetisation variance was determined. Generally 1 to 3 specimens from each sample were treated to stepwise thermal demagnetisation, using a Magnetic Measurements Ltd thermal demagnetiser, in 50-40°C steps up to 700°C. Low frequency magnetic susceptibility (K_{lf}) was monitored after heating stages, measured using a Bartington MS2B sensor. Specimens from the Bishops Court Quarry gave poor quality results and sister specimens were partly treated to a combination of thermal and alternating field (AF) demagnetisation, the latter conducted using a Molspin tumbling AF demagnetiser. In total 166 and 78 paleomagnetic specimens were demagnetised from the Aylesbeare Mudstone and Exeter groups respectively. The bedding dips in the Aylesbeare Mudstone Grp are 5-10^{o} in an easterly direction, so a fold test was not possible. However, in the Exeter Grp dips are more variable and up to 40^{o}, so a tilt-test was possible

Characteristic remanent magnetisation (ChRM) directions were isolated using principal component-based statistical procedures as implemented in LINEFIND, which uses the measurement variance along with rigorous statistical procedures for identifying linear and planar structure in the demagnetisation data (Kent *et al*. 1983). Both linear trajectory fits and great circle (remagnetisation circle) data were used in defining the paleomagnetic behaviour, guided by objective and qualitative selection of the excess standard deviation parameter (ρ), which governs how closely the model variance, used for analysis, matches the data measurement variance (Kent *et al*. 1983). The PMAGTOOL software (available at https:\\www.lancs.ac.uk\staff\hounslow\default.htm) was used for the analysis of mean directions and virtual geomagnetic poles.

Progressive isothermal remanent magnetisation (IRM) up to 4 T was applied to a representative sub-set of specimens, to investigate the magnetic mineralogy. Thermal demagnetisation of a three component IRM was used to investigate the unblocking and alteration temperature behaviour (Lowrie 1990). A small set of specimens were measured for magnetic hysteresis (maximum field 0.9 T) and thermomagnetic curves (maximum field 300 mT, in air on VFTB). Selected thin sections were investigated to assess the petrography of the Fe-oxides. The anisotropy of magnetic susceptibility (AMS), of selected specimens, was measured using an Agico KLY3S Kappameter, to assess the preservation of the detrital sedimentary fabric (Løvlie & Torsvik 1984; Tarling & Hrouda 1993), and to assess if any fabric has been imparted by tectonism.

Magnetic Mineralogy

Changes in the NRM intensity and K_{lf} of specimens are broadly related to:

a) The amount of silt and clay, with those samples having larger amounts of silt and clay, generally having larger NRM intensity and K_{lf}. For example, aeolian sandstones such as those in the Dawlish Sandstone Fm, have significantly lower NRM intensity and K_{lf} (Fig. 5, see supplementary data). In the Aylesbeare Mudstone Grp red mudstones possess average NRM intensity and K_{lf} of 5.0 mA/m and 20.0 x10^{-6} SI respectively, compared to means of 1.8 mA/m and 7.2 x10^{-6} SI in the red sandstone beds.

b) Reddened and non-reddened samples of the same lithology often possesses dramatically different NRM intensity and K_{lf}; with the non-reddened samples typically having lower values. For example grey, green and white sandstones in the Aylesbeare Mudstone Grp have mean NRM intensity and K_{lf} of 0.9 mA/m and 4.4 x10^{-6} SI respectively.

c) The average NRM intensity and K_{lf} shows progressively large values into the Oddicombe Breccia and Watcombe formations (see supplementary data). This may relate to a progressive increase in volcanic-derived detritus (hence haematite content) in the older units which is mirrored in the Cs content (Merefield *et al.* 1981).

Specimens analysed do not saturate in IRM fields up to 4 T (Fig. 6A,C), indicating that canted antiferrimagnetic minerals (haematite or goethite) are important magnetic minerals. Durrance *et al.* (1978) also detected haematite as the main Fe-oxide in the Littleham Mudstone Fm, with the addition of significant amounts of superparamagnetic haematite. Thermomagnetic curves were nearly reversible and exhibited Curie temperatures of 657-669°C, and thermal demagnetisation of the IRM, shows that specimens, display blocking temperatures up to 650-700^{o}C (Fig. 6). Bcr ranged between 320 and 710 mT, all suggesting haematite. Although the IRM does not approach saturation by 4 T (Fig. 6B), there is no clear evidence for goethite, since we have high SIRM/k values, and no well-defined Neel temperature for goethite. IRM acquisition below 100 mT is mostly <15% of the 1T IRM, except for aeolian sandstone units in the Dawlish Sandstone Fm, and grey or red mottled green/grey lithologies (Fig. 6A,C,E). Hence, these later types of lithologies have a greater contribution from a low coercivity mineral, probably magnetite. In specimens DS16, (from Dawlish Sandstone Fm aeolian sandstones) and L3 (grey sandstone, Littleham Mudstones Fm) the low coercivity remanence demagnetises by 450^{o}C- 550^{o}C, which could suggest an oxidized, or Ti-rich magnetite (Fig. 6F). The >300 mT coercivity component in specimen DS16 has a blocking temperature of ~550^{o}C, probably due to a pigment-dominated haematite remanence (Turner 1979) in this sample.

Petrography indicates, like other red-beds, that the haematite is present as two phases, firstly sub-micron haematite (pigmentary haematite), which coats pore perimeters and is often internal to some rock clasts, secondly as larger specular haematite particles, most obvious as detrital opaque grains (Turner 1979; Fig. 3E). The pore-lining pigmentary haematite is multiphase in origin, since it both coats feldspar overgrowths, and to a lesser extent, coats the grains prior to the overgrowths (observed in Dawlish Sandstone Fm only). Compaction related pressure solution at some grain contacts, shows greater amounts of pigment coating the pores, and lesser amounts between the grain contacts, demonstrating both pre and post-compaction pigmentary haematite formation, with probably the bulk of the pigment produced post compaction. Some of the pigmentary haematite may have formed pre-deposition, since it is widely dispersed within a variety of siltstone and phyllite clasts.

The specular haematite is dominated by detrital opaques, which are either present as haematite dominated particles, or compound particles in-part composed of other silicate minerals. The compound particles are occasional haematised clastic rock fragments (intraformational?) but most are of uncertain origin (Fig. 3E). These two types of specularite grains vary in abundance from about 1% to trace amounts. Larger amounts tend to occur in samples that are finer-grained or less well sorted, and lesser amounts typically in the well-sorted aeolian sandstones.

Magnetic Fabric

The anisotropy of magnetic susceptibility (AMS) overall shows a primary depositional magnetic fabric, characterised by vertical-to-bedding K_{min} directions (Figs. 7 a-d) and largely oblate (T >0) fabrics (Figs. 7 e - h). The mudstones have the stronger AMS (greater P values) and are always oblate. The sandstones within the Aylesbeare Mudstone Grp and the various breccia units show more variable AMS fabrics ranging into the prolate fields (T <0), especially so for some sandstones from the breccia units (Fig. 7e,h). This may relate to the more poorly sorted, probably more chaotically deposited grains in the breccia units (possibly related to mudflow deposition, *cf.* Park *et al.* 2013). K_{max} axis trends (Figs. 7I to l) for specimens from the breccia units (Fig. 7l) show both N-S trends and ENE-WSW trends similar to the clast imbrication directions (typically between easterly and northerly directions) of Laming (1982) and Selwood *et al.* (1984). This demonstrates the K_{max} directions parallel the fluvial transport directions. The N-S K_{max} axes trends are common near the Babbacombe-Torquay promontory and in the Teignmouth Breccia Fm. Similar easterly and northeasterly K_{max} axes trends are present in the Exmouth Sandstones and Mudstones, whereas those in the Littleham Mudstone Fm are more variable.

The specimens from aeolian sandstones (from the Dawlish Sandstone Fm and upper part of the Teignmouth Breccia Fm) show a larger proportion of prolate fabrics (T <0) with many more K_{min} axes deviating from vertical (Figs. 7c, g). This is partly due to the lower susceptibility of these samples, so that the strength of the AMS is closer to the sensitivity limits of the KLY3S. However, it is also a reflection of the rolling grain transport on the leeward slip-faces of the aeolian dunes (Ellwood & Howard 1981), producing a grain long-axis orientation transverse to the average wind direction (Schwarzacher 1951), which was to the NW to NNW (Laming 1982; Newell 2001). This is clearly shown in the specimens from the Bishops Court Quarry in which the K_{max} axes are transverse to the aeolian foresets (Edwards & Scrivener 1999).

Mineralogical origin of magnetic properties

In summary, the magnetisation in these units is dominantly carried by haematite, with a likely large range of grain size from superparamagnetic (pigmentary) haematite to larger (specularite) particles of remanence carrying haematite. A strong control on the concentration of haematite is related to the clay and silt content, and perhaps also the concentration of volcanic rock detritus. The pigmentary haematite appears to have a multiphase origin, ranging from possible pre-deposition to late diagenetic, a typical feature of European Permian red beds (Turner *et al.* 1995;

1999). Largely detrital, specular haematite, varies in amounts relating to the degree of sediment sorting and the sediment supply. In the breccia units the maximum susceptibility axes reflect palaeocurrent-parallel trends, shown by clast imbrication directions. In aeolian transported sediments, the transverse trends in K_{max} axes reflect lee-face transport on dune slip faces. In the lacustrine mudstones the K_{max} directions may represent wave-produced (or perhaps wind-related?) grain orientations in the lake playa systems hence, the AMS shows a primary depositional fabric, probably carried mostly by haematite.

Palaeomagnetic Results

The majority of the 250 specimens demagnetised show little change in K_{lf} during demagnetisation, although the mudstones (particularly from the Littleham Mudstone Fm), tend to show alteration at >600^{o}C, with lower temperature alteration in some specimens (Fig. 6). In some specimens, this alteration obscures the recovery of the remanence at higher demagnetisation temperatures.

Demagnetisation isolates two remanence components. Firstly, a positive, often northerly, steeply inclined component (Component A), between room temperature and often up to 350^{o}C, but sometimes up to 500-600°C (Fig. 8). This component is more northerly in specimens from the Aylesbeare Mudstone Grp (Fisher mean, 005^{o}, +59^{o}, k= 7.7, Ns=135), but more southerly in specimens from the Exeter Grp (Fisher mean, 010^{o}, +82^{o}, k=6.7, Ns=44; see supplementary data). This component is more prevalent in the Aylesbeare Mudstone Grp (79% of specimens) compared to the Exeter Grp (56% of specimens), in which it is most prevalent in specimens from the Dawlish Sandstone Fm. It does not correspond in direction particularly well to the expected modern dipole field (i.e. inclination of 68^{o}) and probably represents a composite component comprising mostly a Brunhes (viscous?) magnetisation plus the characteristic remanence. In 10% of samples from the Aylesbeare Mudstone Grp, this was the only component present. In the Exeter Grp 15% of specimens are dominated by this component, the bulk of these being from the Dawlish Sandstone Fm.

A second component is recognised between about 400 and 650-700 °C that is a northerly, positively inclined or southerly, negatively inclined direction (Fig. 8), interpreted as the characteristic remanence (ChRM). In the Littleham Mudstone Fm the unblocking temperature range of this component is mostly above 500^{o}C- 600^{o}C, whereas in specimens from the Exeter

Grp, the unblocking of the ChRM often starts at temperatures of ~400°C. Some 52% of specimens (49% in Aylesbeare Mudstone Grp and 57% in Exeter Grp) had suitable linear trajectory ChRM line fits (here termed 'S-type' data; Fig. 8). This S-type demagnetisation behaviour was visually classified into three quality classes, S1, S2 and S3 (Figs. 8, 9). The mean α_{95} linear fits and ρ for these classes indicate the generally larger model variance required to accommodate the less quality line-fits (see supplementary data). Average confidence cone angles for these line-fit classes vary from 3.2 to 13.9°. The mean directions for the ChRM line-fits pass the reversal test (McFadden & McElhinney 1990), for all except the Littleham Mudstone Fm (Table 1; Fig. 9a).

Some 28% of specimens displayed great circle trends, of varying arc length, towards interpreted Permo-Triassic reverse and normal polarity directions (here referred to as T-type demagnetization behaviour; Fig. 8). This T-type behaviour was visually classified into three quality classes, T1, T2 and T3, based on the visual length and scatter of the demagnetisation points about the great circle, with T1 being the best quality. The mean α_{95} for the poles to the fitted planes, for these three data classes range from 9 to 20° (see supplementary data). These great circle fits included the origin in 67% of these cases.

Data from the Dawlish Sandstone Fm yield the least well-defined results, particularly those from Bishops Court Quarry, which are dominated by component A overprints. These samples also display mainly low blocking temperatures (i.e. the NRM is largely demagnetised by ~500°C). Some specimens from this locality could be AF demagnetised indicating that either these sandstones originally had no haematite, or more likely a substantial proportion of haematite had been removed, possibly by Quaternary ground water flow (e.g. Johnson *et al.* 1997). Notably, those samples that did not retain a ChRM, generally lacked specular haematite particles in thin section, whereas samples of aeolian sandstone which possessed a ChRM often possessed specularite in small amounts. Hence, the poor palaeomagnetic behaviour in the Bishops Court Quarry samples is due to a paucity of specularite, and the dominance of pigment-dominated magnetisations, not unlike other Permian aeolian sandstones such as the Penrith Sandstone (Turner *et al.* 1995).

Mean directions and paleopoles

As well as the conventional means using the ChRM directions, mean directions were also determined using 'specimen-based' means, by combining the great circle paths with the specimen line-fit ChRM (Table 1), to produce combined means using the method of McFadden & McElhinney (1988). This method determines a mean direction, by including the 'fixed-point' ChRM directions, and those points on the projected great circles, which maximise the resultant length (i.e. in effect those calculated points on the great circle which are closest to the combined mean direction). These means are broadly similar to the line-fit ChRM means, except that for the Dawlish Sandstone and Exe Breccia, which have steeper inclination and greater dispersion (Table 1). The great-circle combined means pass the reversal test for the Littleham Mudstone Fm, Exmouth Mudstone and Sandstone Fm, and Dawlish Sandstone plus Exe Breccia formations (Table 1). Using the line-fit ChRM directions alone, the combined mean directions for the Aylesbeare Mudstone and Exeter groups pass the reversal test (Table 1).

Fold tests used the S-class ChRM directions for the Exeter Grp from the coastal sections. These pass the fold test indicating the pre-tilting nature of the magnetisations (Fig. 9b). The fold test of McFadden (1990) produced an f-statistic ($F_{[6,82]}$) of 1.90. Likewise these data pass the DC fold test of Enkin (2003), with best unfolding at 93.5%, with a 95% confidence interval ±25.2%. A progressive unfolding test (Watson & Enkin 1993) indicated best unfolding at 78%, with 95% confidence intervals on the unfolding% of 34% to 114% (Fig. 9b).

The virtual geomagnetic pole (VGP) data is consistent with other Permian data from stable-Europe, confirming the Permian age of these magnetisations. The mean direction for the Exeter Grp produces a virtual geomagnetic pole (VGP) similar to stable-Europe sediments from the youngest part of the KRPS (see Supplementary Data), although the mean is slightly to the east of the European apparent polar wander path of Torsvik & Cocks (2005). The Exeter Volcanic Rocks VGP of Zijderveld (1967) is similar to that from the Aylesbeare Mudstone Grp (Table 1), whereas the VGP pole for the Exeter Grp sediments from this study, is displaced slightly more to the east (see Supplementary Data).

Magnetostratigraphic Interpretation

The line-fit ChRM directions from the Aylesbeare Mudstone Grp (and Exe Breccia Fm) were converted to virtual geomagnetic pole (VGP) latitude using the line-fit ChRM mean in Table 1

(Figs. 10a,b (iii)). For those specimens that had no line-fit, the point on their great circle nearest this mean, were used for calculating the VGP latitude (Fig. 10). All specimens were also assigned a polarity quality (Fig. 10a,b (ii)) based on the quality of demagnetisation behaviour and, if from T-class specimens, the length and end point position of the great circle trend (similar to the procedures used by Ogg & Steiner 1991; Hounslow & McIntosh 2003). One specimen of good-quality polarity (i.e. S-Type) was sufficient to define the horizon polarity, whereas with specimens of poorer quality at least two are required (Figs. 4, 10). Some 12% of specimens failed to yield data which could be used to determine horizon polarity (10% in Aylesbeare Mudstone Grp, 15% in Exeter Grp) and eight horizons failed to yield any specimens which could reliably be used to determine magnetic polarity (Figs. 4, 5). Most of these are from sandstones, with most of these in the Dawlish Sandstone Fm at Bishops Court Quarry (Fig. 4).

All the samples collected from below the Exe Breccia Fm are of reverse polarity, with those sections situated stratigraphically above the Langstone Rock outcrop having both reverse and normal polarity (Figs. 4, 5). The single sample from the Knowle Sandstone Fm (Fig. 2; Table 1) likewise confirms the reverse polarity results from the age-equivalent Exeter Volcanic Rocks found by Creer (1957), Zijderveld (1967) and Cornwall (1967). Significantly, two sites in the Torbay Breccia Fm sampled in the reconnaissance study of Cornwall (1967) produced reverse polarity, suggesting that reverse polarity probably dominates to the base of the Exeter Grp.

Major magnetozone reverse and normal couplets have been numbered (Fig. 10) from the base of the first normal polarity samples in the Exe Breccia Fm, using the prefix EA (for Exeter-Aylesbeare). The magnetic polarities of six magnetozones are defined with multiple specimens from a single sampling horizon (EA3n.1r, EA3n.2r, EA5n.1r), and EA3r.1n is defined with a single specimen of S-class behaviour (Fig. 10).

Discussion

The major geomagnetic polarity marker in the Permian is the end of the Kiaman reverse polarity Superchron, which has been comprehensively studied since the 1950's in Russian successions (Molostovsky 1983; Burov *et al*. 1998). Studies on marine fossil-bearing rocks which demonstrate the end of the Kiaman superchron are discontinuous studies in the SW USA (Steiner, 2006), and Japan (Kirschvink *et al.* 2015), along with studies on successions in China (Steiner *et al*. 1989; Embleton *et al*. 1996). The overlying reverse and normal polarity Illawarra

Superchron, has been extensively investigated in marine successions in the Salt Range in Pakistan, China and Iran (Haag & Heller 1991; Gallet *et al*. 2000; Jin *et al*. 2000; Steiner 2006), along with flood-basalts in China (Ali *et al*. 2002; Zheng *et al.* 2010). Studies on non-marine rocks from the Illawarra Superchron have been extensive in Russia, on outcrop and borehole material (Molostovsky 1983; Burov *et al*. 1998) and core material from the Southern Permian Basin (Menning et al. 1988; Nawrocki 1997; Turner *et al*. 1999; Lawton *et al*. 2003; Szurlies 2013). These studies together allow the magnetic polarity stratigraphy (Fig. 11) to be defined through the Roadian to Changhsingian (Steiner 2006; Hounslow submitted). The base of the Illawarra superchron is in the lower to mid Wordian based on magnetostratigraphic data from the Grayburg Fm in Texas and New-Mexico (Steiner 2006) and limestones from Japan (Kirschvink *et al.* 2015).

Magnetostratigraphic studies in the southern Permian Basin well Mirow 1/1a/74 (Menning et al. 1988; Langereis *et al*. 2010), and wells in Poland (Nawrocki 1997) show a long-duration reverse polarity interval (equivalent to MP3r –UP1r interval) with under and overlying mixed polarity-intervals (Fig. 11). The normal magnetozones in the Lower Drawa Fm and Havel Subgroup are probably equivalent with the MP1n to MP3n interval in the GPTS of Hounslow (submitted). Equivalent normal magnetozones in the Notec and Hannover formations are more fully represented by studies from the Lower Leman Sandstone from the Johnston and Jupiter field in the southern North Sea (Turner *et al.* 1999; Lawton & Roberson 2003). These correlations are constrained by the overlying Zechstein, and indicate that the Zechstein successions are entirely Changhsingian in age, rather than as old as early Wuchiapingian, as suggested by the conodonts *Merrillina divergens* and *Mesogondolella britannica* (Korte *et al.* 2005; Legler *et al*. 2005; Słowakiewicz *et al*. 2009), and the synthesis of Szurlies (2013). Like the magnetostratigraphic interpretation here, Sr-isotope data indicates a short duration for the Zechstein of ~ 2Ma, with a likely age range of 255-251.5 Ma, placing it firmly in the Changhsingian (Denison & Peryt 2009). Various attempts at dating the Kupferschiefer at the base of the Zechstein (Z1 cycle) have failed to yield consistent results, with Re-Os ages giving wide 95% confidence intervals (Pašava *et al.* 2010).

Four pieces of information have allowed dating of the Exeter Grp succession to the Permian.

1) Volcanic units interbedded with the Knowle Sandstone of the Exeter area, and similar units equivalent to the Thorverton Sandstone and Bow Breccia in the Crediton Trough, have Ar-Ar

ages of 291- 282 Ma (Edwards & Scrivener 1999). Volcanic clasts in the breccia units give Ar-Ar dates of 280 Ma. This suggests the volcanism and associated interbedded sediments are late Sakmarian through to late Artinskian in age, using the timescale of Henderson *et al.* (2012).

2) The Dartmoor Granite has Rb-Sr, U-Pb and Ar-Ar ages of 280 ±1 Ma (Scrivener 2006), placing its formation in the latest Artinskian (timescale of Henderson *et al*. 2012). Clasts of the granite begin to occur in the unroofing succession in the Teignmouth and Heavitree Breccias (Dangerfield & Hawkes 1969; Edwards *et al*. 1997), indicating that these units were deposited some millions of years after the granite formation, in order to allow the granite to be unroofed.
3) Miospore assemblages containing *Lueckisporites virkkiae*, occur from the Whipton Fm, around Exeter, but also in younger units in the Crediton Trough, equivalent to the Alphington and Heavitree Breccias (Edwards *et al*. 1997). Assemblages containing this miospore are widespread in European Zechstein deposits and similar 'Thuringian' and Russian Tatarian assemblages (Visscher 1973; Utting 1996). In the northern hemisphere, *Lueckisporites virkkiae* has its first appearance in the early Roadian (lower Kazanian in Russia; Utting 1996) to latest Kungurian (Shu 1999; Mangerud 1994) with youngest ranges into the latest Changhsingian.
4) The foot-print trace-fossil *Cheilichnus bucklandi*, found in the Dawlish Sandstone near Exeter (Edwards *et al*. 1997) suggests equivalence to the Germanic 'Rotliegend' (McKeever & Haubold 1996). However, this genus is restricted to aeolian dune units and is probably only vaguely indicative of the Permian (Lucas & Hunt 2006).

Constraints on the youngest possible age of the Aylesbeare Mudstone Grp are magnetostratigraphy and vertebrate fossils from the overlying Otter Sandstone Formation (Hounslow & McIntosh 2003; Benton 1997), which indicate the Sherwood Sandstone Grp is as old as early Anisian (Middle Triassic), and probably ranges down into the Olenekian of the Lower Triassic (Hounslow & McIntosh 2003; Hounslow & Muttoni 2010). Based on regional climate comparisons between the Budleigh Salterton Pebble Beds and the 'Conglomérate principal' of the Vosges region in NE France, Durand (2006) suggests a probable Smithian age (early Olenekian) for the Budleigh Salterton Pebble Beds Fm, consistent with the magnetostratigraphy.

This work indicates that the oldest normal magnetozone detected is in the mid-parts of the Exe Breccia (i.e. EA1n), with a substantial thickness (perhaps up to ~1 to 1.5 km) of reverse polarity in the underlying parts of the Exeter Grp. Although we cannot locate the base the EA1n (hence equivalent MP1n) precisely due to lack of suitable outcrop, this normal magnetozone is the earliest evidence (equivalent to early MP2n, or normal polarity part of MP1) of the Illawarra Superchron (Fig. 11). There may be up ~55 m unsampled in the interval between our outcrops at this boundary. The end of the KRPS provides an important age tie point (267.1±0.8 Ma; Hounslow submitted) to the early-mid Wordian in the Middle Permian (Guadalupian). The oldest occurrence of the *Lueckisporites virkkiae* assemblage is found in the Whipton Fm, which suggests that this formation could be as old as early Roadian or latest Kungurian (~272 Ma; Henderson *et al.* 2012). This would give a minimum of ~8 Ma after formation of the Dartmoor Granite for exhumation of the granite and for the first granite detritus to appear in the Teignmouth- Heavitree breccias.

The overlying normal polarity magnetozone EA3n, is therefore likely to be equivalent to the MP3n normal magnetozone in the upper and mid parts of the Capitanian (Fig. 11). The EA3r magnetozone is equivalent to the MP3r to UP1r interval (in the lower part of the Wuchiapingian), with the overlying normal magnetozones (i.e. EA4n to EA5n) equivalent to those in the upper parts of the Wuchiapingian to basal Changhsingian (Fig. 11). Reverse magnetozone EA2r, in the top of the Exe Breccia is probably the equivalent of MP2r in the basal Capitanian. Sub magnetozone EA3r.1n in the Littleham Mudstone Fm is probably equivalent to UP1n in the Wuchiapingian.

Alternative Lower Triassic age models?

The alternative Lower Triassic age of the Aylesbeare Mudstone Grp suggested by Warrington & Scrivener (1990) and Edwards *et al*. (1997), is untenable using the magnetostratigraphy. To test their hypothesis, the most likely early Triassic correlation model suggests that EA3n is the age equivalent of the first Triassic magnetozone, LT1n (Fig. 11), with the overlying EA3r to EA5n interval extending into the earliest Olenekian, an interval of some 1.4 Ma (Hounslow & Muttoni 2010). However, this seems unlikely for the following reasons:

1) The local clast lithologies (e.g. murchisonite) seen in the breccia at the base of the Littleham Mudstone Fm, are similar to those in the Exeter Grp, and very different to those found in the

Budleigh Salterton Pebble Beds and other Lower Triassic units further north in the UK, which contain Armorican-derived clasts and grains (Cocks 1993; Morton *et al.* 2013).

2) It would require a minimum hiatus of ~ 13-15 Ma between the Exe Breccia and the Aylesbeare Mudstone Grp, which seems unlikely considering the apparently conformable nature of the boundary between these formations.
3) If the hypothesis of Warrington & Scrivener (1990) was correct a prediction would be numerous normal polarity intervals (from the Illawarra superchron) below the Aylesbeare Mudstone Grp, but we have only found these in the Exe Breccia Fm with no evidence of normal polarity in the underlying *c*.1 km of the Exeter Grp.
4) The Lower Triassic model would suggest a ~1.4 Ma duration for the EA3n to EA5n interval requiring very large accumulation rates, comparable to the deepest grabens in the Southern Permian Basin, north of the Variscan front, which there contain substantial thicknesses of Zechstein.

Wider regional implications

A consequence of these data, is that it is now possible to assess the relationship of these SW England successions to the much better studied Rotleigend-II group in the Southern Permian Basin (Fig. 11). The magnetostratigraphy suggests a similarity in age of the Altmark unconformities with the Devon Permian sequence boundaries. The magnetic polarity stratigraphy from the Mirow, Czaplinek and Piła wells suggests that the Altmark III unconformity is roughly equivalent to the base of the Littleham Mudstone Fm (base of Pm5), Altmark II, with the base of Pm4 (Figs. 2, 11). Less certain is the correlation of the base of unit B in the Littleham Mudstone Fm, with Altmark IV. The base of Pm3 probably relates to the Altmark I unconformity, which separates the Muritz Subgroup from the Havel Subgroup, across the Saalian unconformity, since underlying successions both contain volcanic units.

The calcrete and rhizoconcretion bearing sandstone, in the uppermost part of the Straight Point Sandstone Mbr, is unusual in that no other well developed palaeosols are seen in the remainder of these Permian successions. It is not until the mid Triassic (Anisian) Otter Sandstone Fm, that calcretes begin to be widely developed in SW England. The Capitanian-Wuchiapingian boundary was an interval with dramatic, but poorly understood shifts in the global carbon cycle (Nishikane *et al.* 2014). A tentative reason for this palaeosol development is the rapid warming associated with increased CO_2 in the atmosphere (and associated increased evaporation rates to create calcretes; Alonso-Zarza 2003), that developed after the extinction at the Capitanian-Wuchiapingian boundary. The peak is associated with a negative $\delta^{13}C$ excursion (Chen *et al.* 2011; Nishikane *et al.* 2014) in the early Wuchiapingian, which corresponds closely to the early parts of MP3r (Zheng *et al.* 2010; Fig. 11).

The dramatic switch between breccia-dominated facies of the Exeter Grp to the mudstone-dominated facies of the Aylesbeare Mudstone Grp, occurs within the early Capitanian (Fig. 11). We tentatively relate this switch in regimes to the Kamura cooling event (seen as a large positive $\delta^{13}C$ excursion during the Capitanian), which began in the early Capitanian (Isozaki *et al.* 2011). This has been associated with lows in atmospheric CO_2, and cooler oceanic surface waters in both the Panthalassa and Paleo-Tethys Oceans (Isozaki *et al.* 2011; Nishikane *et al.* 2014). This cooling event may have allowed more moisture bearing weather systems to penetrate further northwards into the heart of Pangaea, from the Paleo-Tethys, so allowing greater delivery of mud into the playa systems of the Aylesbeare Mudstone Grp.

The Southern Permian Basin, Parchim and Mirow formations shows a number of similarities to the Devon successions. The Parchim Fm dominantly comprises thick conglomeratic braidplain-type deposits, extending to sandflat and locally playa mudstone deposits in the basin centre (McCann 1998; Rieke *et al.* 2003). Tectonic control of facies was important during the Parchim Fm. Like the Exeter Group in sequence Pm3 the Parchim Fm has an earlier wetter phase and a later dryer phase (Rieke *et al.* 2003). This is overlain by the Mirow Fm which is characterized by the progradation of sand-prone fluvial facies with frequent claystones, over a much wider extent in the Southern Permian Basin than the Parchim Fm. The rarity of conglomerates (except at basin margins), with instead claystones (containing fossils indicative of freshwater conditions) and sand-prone facies dominating, is very different to the Parchim Fm (McCann 1998). Hence, the start of the Mirow Fm sees a switch to climatically wetter conditions (Rieke *et al.* 2003), like seen in the Aylesbeare Mudstone Grp. The coincidence in timing and the switch to wetter environmental conditions, seen in the Devon successions and German basins, suggests these major facies changes are climatically controlled.

Conclusions

The palaeomagnetic signal in the Exeter and Aylesbeare Mudstone groups is carried by haematite, whose mean directions pass the reversal test. The remanence in the Exeter Grp passes a fold test. On the basis of the AMS, the fabric carried by haematite is detrital in origin. Reverse polarity dominates in the lower part of the Exeter Grp, with the start of the Illawarra superchron, in the early Wordian, identified in the Exe Breccia Fm. Five normal-reverse couplets are found in the overlying sediments starting in the upper part of the Exe Breccia Fm (Langstone Mbr) and into the Aylesbeare Mudstone Grp. This magnetostratigraphic data allow the Exmouth Mudstone and Sandstone Fm to be dated to the Capitainian to the earliest Wuchiapingian, and the overlying Littleham Mudstone Fm dated to the earliest Wuchiapingian, through to the an age near the Wuchiapingian-Changhsingian boundary. The Permian successions in SW England successions are now the most precisely dated Permian succession in the UK, and should provide a foundation for the better understanding of other UK Permian basins. The similarity in the timing between sequences here, and those of the Rotliegend-II Group in the Southern Permian Basin, indicates that palaeoclimatic change is a fundamental metric in their subdivision. The question of the position of the Permo-Triassic boundary in SW England has now been effectively resolved, and ironically, now corresponds to the position taken by Victorian geologists such as Irving (1888).

Acknowledgements

This work was part-funded by a British Geological Survey- University collaboration grant. Richard Scrivener led fieldwork to the Crediton Trough, and Paulette Posen assisted during fieldwork to the Exeter Grp. Robert Hawkins and Laurence Thistlewood measured some of the samples. Sylvie Bourquin and Antoine Bercovici assisted in the fieldwork in 2007. Simon Chew drafted some of the figures. The MOD kindly allowed access to the Straight Point firing range.

References

Ali, J.R, Thompson, G.M., Song, X. & Wang, Y. 2002. Emeishan Basalts (SW China) and the 'end-Guadalupian' crisis: magnetobiostratigraphic constraints. *Journal of the Geological Society*, **159**, 21-29.

Alonso-Zarza, A. M. 2003. Palaeoenvironmental significance of palustrine carbonates and calcretes in the geological record. *Earth-Science Reviews*, **60**, 261-298.

Barton, C. M., Woods, M. A., Bristow, C. R., Newell, A. J., Westhead, R. K., Evans, D. J., Kirby, G. A., & Warrington, G. 2011. *The geology of south Dorset and south-east Devon and its World Heritage Coast.* Special Memoir of the British Geological Survey, Sheets 328, 341/342, 342/343 and parts of 326/340, 327, 329 and 339. HMSO

Bateson, J.H. & Johnson, C.C. 1992. *Reduction and related phenomena in the New Red Sandstone of south-west England*, British Geological Survey, Technical report WP/92/1.

Benton, M.J., Cook, E., & Turner, P. 2002. *Permian and Triassic red beds and the Penarth Group of Great Britain*. Geological Conservation Review Series. Joint Nature Conservation Committee, Peterborough.

Benton, M. J. 1997. The Triassic reptiles from Devon. *Proceedings of the Ussher Society*, **9**, 141-152.

Burov, B.V., Zharkov, I.Ya, Nurgaliev, D.K., Balabanov, Yu. P., Borisov, A.S. & Yasonov, P.G. 1998. Magnetostratigraphic characteristics of Upper Permian sections in the Volga and the Kama areas. *In:* Esaulova, N.K., Lozonsky, V.R., Rozanov, A.Yu. (eds). *Stratotypes and reference sections of the Upper Permian in the regions of the Volga and Kama Rivers*. Moscow, GEOS.

Butler, M. 1998. The geological history and the southern Wessex Basin- a review of new information from oil exploration. *In:* Underhill, J.R. (ed.), *Development, evolution and petroleum geology of the Wessex Basin*. Geological Society London Special Publication **133**, 67-86.

Chapman, T. J. 1989. The Permian to Cretaceous structural evolution of the Western Approaches Basin (Melville sub-basin), UK. *In:* M.A. Cooper (ed.), *Inversion Tectonics,* Geological Society, London, Special Publications; **44**, 177-200.

Chen, B., Joachimski, M. M., Sun, Y., Shen, S. & Lai, X. 2011. Carbon and conodont apatite oxygen isotope records of Guadalupian–Lopingian boundary sections: Climatic or sea-level signal? *Palaeogeography, Palaeoclimatology, Palaeoecology*, **311**, 145-153.

Cocks, L.R.M. 1993. Triassic pebbles, derived fossils and the Ordovician to Devonian palaeogeography of Europe. *Journal Geological Society London*, **150**, 219-226.

Cornwall, J.D. 1967. Palaeomagnetism of the Exeter Lavas, Devonshire. *Geophys. Journal Royal Astro. Soc.*, **12**, 181-196.

Dangerfield, J. & Hawkes, J. R. 1969. Unroofing of the Dartmoor Granite and possible consequences with regard to mineralization. *Proc. Ussher Soc.,* **2**, 122-131.

Denison, R. E. & Peryt, T. M. 2009. Strontium isotopes in the Zechstein (Upper Permian) anhydrites of Poland: evidence of varied meteoric contributions to marine brines. *Geological Quarterly*, **53**, 15

Durand, M. 2006. The problem of the transition from the Permian to the Triassic Series in southeastern France: comparison with other Peritethyan regions. *In:* Lucas, S.G., Cassinis,

G. & Schneider J.W. (eds) *Non-Marine Permian Biostratigraphy and Biochronology*, Geological Society, London, Special Publications, **265**, 281-296.

Durrance, E. M., Meads, R. E., Ballard, R. R. B. & Walsh, J. N. 1978. Oxidation state of iron in the Littleham Mudstone Formation of the new red sandstone series (Permian-Triassic) of southeast Devon, England. *Geological Society of America Bulletin*, **89**, 1231-1240.

Edwards, R.A. & Scrivener, R.C., 1999. *Geology of the country around Exeter. Memoir of the British Geological Survey, Sheet 325 (England and Wales)*, London, HMSO.

Edwards, R.A., Warrington, G., Scrivener, R.C., Jones, N.S., Haslam, H.W. & Ault, L. 1997. The Exeter Group, south Devon, England: a contribution to the early post-Variscan stratigraphy of northwest Europe. *Geological Magazine*, **134**, 177-197.

Ellwood, B.B. & Howard, J.H. 1981. Magnetic Fabric Development in an Experimentally Produced Barchan Dune. *Journal of Sedimentary Research*, **51**, 97-100.

Embleton, B.J.J., McElhinny, M.W., Zhang Z. & Li Z.X. 1996. Permo-Triassic magnetostratigraphy in China: the type section near Taiyuan, Shanxi Province, North China. *Geophys. J. Int.* **126**: 382–388

Enkin, R.J. 2003. The direction- correction tilt test: an all purpose tilt/fold test for palaeomagnetic studies. *Earth Planet. Sci. Lett*., **212**, 151-166.

Evans, C. D. R. 1990. *The geology of the western English Channel and its western Approaches. UK Offshore regional report*. British Geological Survey, HMSO, London.

Gallet, Y., Krystyn, L., Besse, J., Saidi, A. & Ricou, L-E. 2000. New constraints on the upper Permian and Lower Triassic geomagnetic polarity timescale from the Abadeh section (central Iran). *Journal of Geophysical Research*, **105**, 2805-2815.

Gallois, R.W. 2014. The position of the Permo-Triassic boundary in Devon, UK. *Geoscience in South-West England*, **13**, 328-338.

Haag, M. & Heller, F. 1991. Late Permian to Early Triassic magnetostratigraphy: Earth Planet. Sci. Letter, 107, 42-54.

Hamblin, R.J.O., Crosby, A., Alson, R.S., Jones, S.M., Chadwick, R.A., Penn, I.E. & Arthur, M.J. 1992. *United Kingdom off-shore report: the geology of the English Channel*. British Geological Survey, HMSO, London.

Harvey, M.J. Stewart, S.A., Wilkinson, J.J., Ruffell, A. H. & Shall, R. K. 1994. Tectonic evolution of the Plymouth Bay Basin. *Proceedings of the Ussher Society*, **8**, 271-278.

Henderson, C. M., Davydov, V. I. & Wardlaw, B. R. 2012. The Permian Period. *In:* Gradstein, F.M., Ogg, J.G, Schmitz, M.D. & Ogg, G.M (eds), *The geologic time scale 2012*, vol. 2, Elsevier, Amsterdam, 653-679.

Henson, M.R. 1972. The form of the Permo-Triassic basin in south-east Devon. *Proc. Ussher Soc*. **3**, 447-457.

Hounslow, M.W. & McIntosh, G. 2003. Magnetostratigraphy of the Sherwood Sandstone Group (Lower and Middle Triassic): South Devon, U.K.: Detailed correlation of the marine and non-marine Anisian. *Palaeogeogr. Palaeoclimat. Palaeoecol.* **193**, 325-348.

Hounslow M.W. & Muttoni G. 2010. The geomagnetic polarity timescale for the Triassic: Linkage to stage boundary definitions. *In:* Lucas, S.G. (ed) *The Triassic timescale*. Special Publication of the Geological Society, **334**, 61-102.

Hounslow, M.W. (submitted). Palaeozoic geomagnetic reversal rates following superchrons have a fast re-start mechanism. *Nature Communicaions*.

Irving, A. 1888. The red-rock series of the Devon Coast section. *Quart. J. geol. Soc.*, **44**, 149-163.

Isozaki, Y., Aljinovic, D. & Kawahata, H. 2011. The Guadalupian (Permian) Kamura event in European Tethys. *Palaeogeography, Palaeoclimatology, Palaeoecology* **308**, 12–21.

Jin, Y. Shang, Q. & Cao, C. 2000. Late Permian magnetostratigraphy and its global correlation. *Chinese Science Bulletin*, **45**, 698-705.

Johnson, S. A., Glover B. W. & Turner, P. 1997. Multiphase reddening and weathering events in Upper Carboniferous red beds from the English West Midlands. *Journal of the Geological Society*, **154**, 735-745.

Kent, J.T., Briden, J.C. & Mardia, K.V. 1983. Linear and planar structure in ordered mulivariate data as applied to progressive demagnetisation of palaeomagnetic remanence. *Geophysical Journal Royal Astronomical Society*, **81**, 75-87.

Kirschvink, J. L., Isozaki, Y., Shibuya, H., Otofuji, Y. I., Raub, T. D., Hilburn, I. A., Kasuya, T., Yokoyama, M. & Bonifacie, M. 2015. Challenging the sensitivity limits of Paleomagnetism: Magnetostratigraphy of weakly magnetized Guadalupian–Lopingian (Permian) Limestone from Kyushu, Japan. *Palaeogeography, Palaeoclimatology, Palaeoecology*, **418**, 75-89.

Korte, C., Kozur, H. W. & Veizer, J. 2005. $\delta^{13}C$ and $\delta^{18}O$ values of Triassic brachiopods and carbonate rocks as proxies for coeval seawater and palaeotemperature. *Palaeogeography, Palaeoclimatology, Palaeoecology*, **226**, 287-306.

Kostadinova M., Jordanova N., Jordanova D. & Kovacheva M. 2004. Preliminary study on the effect of water glass impregnation on the rock-magnetic properties of baked clay. *Studia Geophysica et Geodaetica*, **48**, 637-646.

Laming, D. J. C. 1966. Imbrications, palaeocurrents and other sedimentary features in the Lower New Red Sandstone, Devonshire, England. *Journal of Sedimentary Petrology*, **36**, 940-959.

Laming, D.J.C. 1969. A guide to the New Red Sandstone of Tor Bay, Petitor and Shaldon. Report *Transaction of Devonshire Association of Science, Literature and Art*, **101**, 207-218.

Laming, D.J.C. 1982. The New Red Sandstone. *In:* Durrance, E.M. & Laming, D.J.C. (eds) *The geology of Devon*. University of Exeter Press, Exeter, 148-178,

Laming, D.J.C. & Roche, D.P. 2013. Faulting in Permo-Triassic strata and buried channels revealed by excavation of the Lympstone-Powderham tunnel, Exe Estuary, Devon. *Geoscience in South-West England*, **13**, 244.

Langereis, C. G., Krijgsman, W., Muttoni, G. & Menning, M. 2010. Magnetostratigraphy - concepts, definitions, and applications. *Newsletters on Stratigraphy*, **43**, 3, 207-233

Lawton, D.E. & Roberson, P.P. 2003. The Johnston Gas Field, Blocks 43/26a, 43/27a, UK Southern North Sea. *In:* Gluyas, J. & Hichens, H.M. (eds), *United Kingdom Oil and Gas Fields, Commemorative Millennium Volume*. Geological Society Memoir, (London) **20**, 749-759.

Legler, B., Gebhardt, U. & Schneider, J.W. 2005. Late Permian non marine to marine transitional profiles in central southern Permian Basin, northern Germany. *Int. Journal of Earth Sciences*, **94**, 851-862.

Leveridge, B.E. Scrivener, R.C. Goode, A.J.J. & Merriman, R.J. 2003. *Geology of the Torquay district, a brief explanation of the geological map sheet 350 Torquay*. Keyworth: British Geological Survey.

Løvlie, R. & Torsvik, T. 1984: Magnetic remanence and fabric properties of laboratory-deposited hematite-bearing red sandstone. *Geophysical Research Letters*, **11**, 229-232.

Lowrie, W. 1990. Identification of ferromagnetic minerals in a rock by coercivity and unblocking temperature properties. *Geophysical Research Letters*, **17**, 159-162.

Lucas, S.G. & Hunt, A.P. 2006. Permian tetrapod foorptints: biostratigraphy and biochronology. *In:* Lucas, S.G. Cassinis, G. & Schneider, J.W. (eds). *Non-marine Permian* *biostratigraphy and biochronology*, Geological Society, London Special Publications, **265**, 179-200.

Mangerud, G. 1994. Palynostratigraphy of the Permian and lowermost Triassic succession, Finnmark Platform, Barents sea. *Review of Palaeobotany & Palynology*, **82**, 317-349.

McCann, T., Pascal, C., Timmerman, M. J., Krzywiec, P., López-Gómez, J., Wetzel, L. & Lamarche, J. 2006. Post-Variscan (end Carboniferous-Early Permian) basin evolution in western and central Europe. *In:* Gee, D. G. & Stephenson, R. A. (eds) *European Lithosphere Dynamics*. Geological Society, London, Memoirs, **32**, 355–388.

McCann, T. 1998. Sandstone composition and provenance of the Rotliegend of the NE German Basin. *Sedimentary Geology*, **116**, 177-198.

McFadden, P. L. 1990. A new fold test for palaeomagnetic studies. *Geophysical Journal International*, **103**, 163-169.

McFadden, P.L. & McElhinney, M.W. 1988. The combined analysis of remagnetisation circles and direct observations in palaeomagnetism. *Earth Planetary Science Letters*, **87**, 161-172.

McFadden, P.L. & McElhinny, M.W. 1990. Classification of the reversal test in palaeomagnetism. *Geophysical Journal International*, **103**, 725-729.

McKeever, P.M. & Haubold, H. 1996. Reclassification of vertebrate trackways from the Permian of Scotland and related forms from Arizona and Germany. *Journal of Paleontology*, **70**, 1011-1022.

McKie, T. & Williams, B.P.J. 2009. Triassic palaeogeography and fluvial dispersal across the northwest European Basins. *Geological Journal*, **44**, 711-741.

Menning, M., Katzung, G. & Lützner, H. 1988. Magnetostratigraphic investigations in the Rotliegendes (300-252 Ma) of Central Europe. *Z. geol. Wiss., Berlin*, **16**, 1045-1063.

Merefield, J.R., Brice, C.J. & Palmer, A.J. 1981. Caesium from former Dartmoor volcanism: its incorporation in NewRed sediments of SW England. *Journal of the Geological Society*, **138,** 145-152.

Molostovsky, E. A. 1983. *Paleomagnetic stratigraphy of the eastern European part of the USSR*. Saratov, University of Saratov [In Russian].

Morton, A.C., Hounslow, M.W. & Frei, D. 2013. Heavy-mineral, mineral-chemical and zircon-age constraints on the provenance of Triassic sandstones from the Devon coast, southern Britain. *Geologos* **19**, 67–85.

Nawrocki, J. 1997. Permian to early Triassic magnetostratigraphy from the central european basin in poland: Implications on regional and worldwide correlations. *Earth. Planet. Sci Lett.,* **152**, 37-58.

Newell, A.J. 2001. Bounding surfaces in a mixed aeolian-Fluvial system (Rotliegend, Wessex Basin, SW UK). *Marine & Petroleum Geology*, **18**, 339-347.

Nishikane, Y., Kaiho, K., Henderson, C. M., Takahashi, S. & Suzuki, N. 2014. Guadalupian–Lopingian conodont and carbon isotope stratigraphies of a deep chert sequence in Japan. *Palaeogeography, Palaeoclimatology, Palaeoecology*, **403**, 16-29.

Ogg, J. G. & Steiner, M. B. 1991. Early Triassic polarity time-scale: integration of magnetostratigraphy, ammonite zonation and sequence stratigraphy from stratotype sections (Canadian Arctic Archipelago). *Earth and Planetary Science Letters*, **107**, 69–89.

Ormerod- Wareing, G. 1875. On the Murchisonite beds of the Estuary of the Exe and an attempt to classify the beds of the Trias thereby. *Quart, J. Geol. Soc. Lond.*, **31**, 346-354.

Park, M. E., Cho, H., Son, M. & Sohn, Y. K. 2013. Depositional processes, paleoflow patterns, and evolution of a Miocene gravelly fan-delta system in SE Korea constrained by anisotropy of magnetic susceptibility analysis of interbedded mudrocks. *Marine and Petroleum Geology*, **48**, 206-223.

Pašava, J., Oszczepalski, S. & Du, A. 2010. Re–Os age of non-mineralized black shale from the Kupferschiefer, Poland, and implications for metal enrichment. *Mineralium Deposita*, **45**, 189-199.

Rieke, H., McCann, T., Krawczyk, C. M. & Negendank, J. F.W. 2003. Evaluation of controlling factors on facies distribution and evolution in an arid continental environment: an example from the Rotliegend of the NE German Basin. *In:* McCann, T. & Saintot. A. (eds) *Tracing Tectonic Deformation Using the Sedimentary Record.* Geological Society, London, Special Publications, **208**, 71- 94.

Roscher, M. & Schneider, J.W. 2006. Permo-Carboniferous climate: Early Pennsylvanian to late Permian climate development of central Europe in a regional and global context. *In:* Lucas, S.G. Cassinis, G. & Schneider, J.W. (eds) *Non-marine Permian biostratigraphy and biochronology*, Geological Society, London Special Publication, **265**, 15-38.

Schwarzacher, W. 1951. Grain orientation in sands and sandstones. *Journal of Sedimentary Research*, 21, 162-172.

Scrivener, R. C., Darbyshire, D. P. F. & Shepherd, T. J. 1994. Timing and significance of crosscourse mineralization in SW England. *Journal of the Geological Society*, 151, 587-590.

Scrivener, R.C. 2006. Cornubian granites and mineralization in SW England. *In:* Brenchley, P.J. & Rawson, P.F. *Geology of England and Wales*. Geological Society of London Publication, Bath, 257-267.

Selwood, E.B. Edwards, R.A., Simpson, S., Chesher, J.A. & Hamblin, R.A. 1984. *Geology of the country around Newton Abbot. Memoir for 1:50,000 geological sheet 339*, British Geological Survey HMSO, London.

Shen, S-Z., Henderson, C.H., Bowring, S.A., Cao1, C-Q. Wang, Y., Wang, W., Zhang, H., Zhang, Y-C. & Mu, L. 2010. High-resolution Lopingian (Late Permian) timescale of South China. *Geological Journal*, **45**, 122–134.

Shu, O. 1999. A brief discussion on the occurrences of *Scutasporites unicus* and *Lueckisporites virkkiae* complexes in the northern hemisphere. *Permophiles*, **33**, 21-23.

Słowakiewicz, M., Kiersnowski, H. & Wagner, R. 2009. Correlation of the Middle and Upper Permian marine and terrestrial sedimentary sequences in Polish, German and USA Western Interior Basins with reference to global time markers. *Palaeoworld*, **18**, 193-211.

Steiner, M. 2006. The magnetic polarity timescale across the Permian-Triassic boundary. *In:* Lucas, S.G. Cassinis, G. and Schneider, J.W. (eds*) Non-marine Permian biostratigraphy and biochronology*, Geological Society, London Special Publication, **265**, 15-38.

Steiner, M.B., Ogg, J., Zhang, Z. & Sun, S. 1989. The Late Permian/early Triassic magnetic polarity time scale and plate motions of south China. *Journal Geophysical Research*, **94**, 7343-7363.

Strachan, R. A., Linnemann, U., Jeffries, T., Drost, K. & Ulrich, J. 2014. Armorican provenance for the mélange deposits below the Lizard ophiolite (Cornwall, UK): evidence for Devonian obduction of Cadomian and Lower Palaeozoic crust onto the southern margin of Avalonia. *International Journal of Earth Sciences*, **103**, 1359-1383.

Szurlies, M., Bachmann, G.H., Menning, M., Nowaczyk, N.R. & Käding, K-C. 2003. Magnetostratigraphy and high resolution lithostratigraphy of the Permian- Triassic boundary interval in Central Germany. *Earth and Planetary Science Letters*, **212**, 263-278.

Szurlies, M. 2013. Late Permian (Zechstein) magnetostratigraphy in western and central Europe. *In:* Gasiewicz, A. & Słowakiewicz, M. (eds) *Palaeozoic climate cycles: their evolutionary and sedimentological impact.* Geological Society, London, Special Publications, **376**, 73-85.

Tarling, D.H. & Hrouda, F. 1993. *The magnetic anisotropy of rocks*. Chapman and Hall, London.

Thomas, H.H. 1909. A contribution to the petrography of the New Red Sandstone in the West of England. *Quarterly Journal of the Geological Society, London*, **65**, 229-245.

Timmerman, M.J. 2004. Timing, geodynamic setting and character of Permo-Carboniferous magmatism in the foreland of the Variscan Orogen, NW Europe. *In:* Wilson, M., Neumann, E.-R., Davies, G.R., Timmerman, M.J., Heeremans, M. & Larsen, B.T. (eds) *Permo-Carboniferous Rifting and Magmatism in Europe*, Special Publication Geological Society, London, **223**, 41-74.

Torsvik T.H. & Cocks L.R.M. 2005. Norway in space and time: A Centennial cavalcade. *Norwegian Journal of Geology*, **85**, 73-86.

Turner, P. 1979. The palaeomagnetic evolution of continental red beds. *Geological Magazine,* **116**, 289-301.

Turner, P., Burley, S.D. Rey, D. & Prosser, J. 1995. Burial history of the Penrith Sandstone (Lower Permian) deduced from the combined study of fluid inclusion and palaeomagnetic data. *In:* Turner, P. & Turner, A. (eds). *Paleomagnetic applications in hydrocarbon exploration*. Geological Society London Special Publications, **98**, 43-78.

Turner, P., Chandler, P., Ellis, D., Leveille, G.P. & Heywood, M.L. 1999. Remanance acquisition and magnetostratigraphy of the Leman Sandstone Formation: Jupiter Fields, southern North Sea. *In:* Tarling, D.H. & Turner, P. (eds) *Palaeomagnetism and diagenesis in sediments*, Geological Society of London special publications, **151**, 109-124.

Ussher, W.A.E 1876. On the Triassic rocks of Somerset and Devon. *Quart Jour. Geol. Soc.*, 32, 367-394.

Ussher, W.A.E 1913. *The geology of the country around Newton Abbott : explanation of sheet 339.* Geological Survey of Great Britain. HMSO.

Visscher, H. 1973. The Upper Permian of western Europe—a palynological approach to chronostratigraphy. *In:* Logan A. & Hills L.V. (eds), *The Permian and Triassic systems and Their Mutual Boundary*. Can. Soc. Pet. Geol. Mem., **2,** 200-219.

Warrington, G. & Scrivener, R.C. 1990. The Permian of Devon, England. *Review Palaeobotany Palynology*, **66**, 263-272.

Watson, G.S & Enkin, R.J. 1993. The fold test in palaeomagnetism as a parameter estimation problem. *Geophysical Research Letters*, **20**, 2135-3137.

Wills, L.J. 1970. The Triassic succession in the central Midlands in its regional setting. *Jour. Geol. Soc. Lond.*, **126**, 225-283.

Zheng, L., Yang, Z., Tong, Y., & Yuan, W. 2010. Magnetostratigraphic constraints on two-stage eruptions of the Emeishan continental flood basalts. *Geochemistry, Geophysics, Geosystems*, **11**, doi:10.1029/2010GC003267.

Zijderveld, J.D.A. 1967. The natural remanent magnetisation of the Exeter Volcanic Traps (Permian, Europe). *Tectonophysics*, **4**, 121-153.

Utting, J., 1996. Palynology of the Ufimian and Kazanian Stages of Russian stratotypes, and their comparison to the Word and Road of Canadian Arctic. *In:* Esaulova, N. K. & Lozovsky, V. R. (eds) *Stratotypes and reference sections of the Upper Permian of regions of the Volga and Kama Rivers*. Izd. “Ecocentr”, Kazan, 486-506.

Figure Captions

Fig. 1. Sketch map of the Permian-Triassic in SE Devon. Inset shows the study location within UK, grey=Lower Palaeozoic basement highs, dotted=Permian basins. SPB=Southern Permian Basin. Numbers correspond to the sampling locations indicated in the Supplementary Data. From Selwood *et al*. (1984) and Edwards *et al*. (1997). Sampling locations on coast indicated by } and in-land as ■.

Fig. 2. The stratigraphy of the Permian- Triassic in the Exeter, and SE Devon coastal area. Based on this work and Laming (1982), Selwood *et al*. (1984), Edwards & Scrivener (1999), Leveridge *et al*. (2003). Thicknesses of the coastal units is based on Selwood *et al*. (1984), Laming (1982) and this work. The chronology is based on Edwards *et al*. (1997), Edwards & Scrivenor (1999) and this work. The Torbay Breccia Formation occurs west of the Stickepath fault zone (SFZ, dashed in grey), and is divisible into an upper unit (the Paignton breccias, PB) probably equivalent to the Oddicombe Breccia Fm , and a lower unit composed of several separate breccias units. PTM=Petit Tor Member. Arrows indicate overstepping units.

Fig. 3. a) The erosional boundary between the Littleham Mudstone Fm (below) and the Budleigh Salterton Pebble Beds Fm (photo courtesy of Richard Porter), b) Immature calcrete and calcretised rootlets, top part of Straight Point Sandstone Member. c) Erosional boundary of breccia (arrowed) at base of the Littleham Mudstone Fm Littleham Cove (photo courtesy of Ian West) Scale arrow height=1.5 m. d) Unconformable boundary (marked in white) between the Watcombe Fm and the Oddicombe Breccia Fm, Whitsands Bay, hammer for scale. E) Detrital opaques (black) and pigmentary haematite grain coating (in red), fluvial sandstone, Dawlish Sandstone Fm, Dawlish Station section. The right hand side opaque (a haematised rock fragment) shows compactional deformation from surrounding framework grains. F) Detrital opaque showing indentation due to compaction into the surrounding quartz grains. Pigmentary haematite rims not present at opaque-quartz boundary. Fluvial sandstone in Dawlish Sandstone Fm. Pore spaces in blue. Scale bar is 100 µm.

Fig. 4. Section logs and summary palaeomagnetic data (horizon polarity, demagnetisation behaviour and specimen polarity) from sections in the Exeter Group. See Fig. 1 for location details. Symbols for specimen polarity and behaviour are larger for better quality behaviour (see

text for details). Ticks adjacent to logs are sampling levels. Sample numbers indicated, for data shown on other figures or in the supplementary data.

Fig. 5. Section logs and summary horizon magnetic polarity data for the stratigraphic section between Lympstone (site 3 on Fig. 1) to the top of the Littleham Mudstone Fm at Budleigh Salterton (Fig. 1). Bed numbers on the log for the Exmouth Mudstones and Sandstones Fm are those of Selwood *et al*. (1984); the divisions in the Littleham Mudstone Fm are from this work (detailed in the supplementary data). Ticks adjacent to logs are sampling levels. Sample numbers indicated, for data shown on other figures or in the supplementary data.

Fig. 6. Isothermal remanent magnetisation curves (A, C, E) and thermal demagnetisation of orthogonal IRM (B, D, F) for representative specimens. Specimen numbers are those shown on Figs. 4 and 5. sst=sandstone; TBF= Teignmouth Breccia Fm, EBF= Exe Breccia Fm.

Fig. 7. Anisotropy of magnetic susceptibility data for the Littleham Mudstone Fm (a, e, i), The Exmouth Mudstone and Sandstone Fm (b, f, j), aeolian sandstones in the Dawlish Sandstone and Teignmouth Breccia formations (c, g, k), and the various breccia units (d, h, l). a),b),c),d), Steroegraphic projections of the specimen K_{max} and K_{min} directions. E), f), g), h) the AMS ellipsoid shape ($T= [2(L_{int}-L_{min})/(L_{max}-L_{min})]-1$; where $L=Ln(K_i)$) and strength ($P = K_{max}/K_{min}$; Tarling & Hrouda, 1993), i),j),k), l), rose diagrams showing the directions of the K_{max} axes, indicating the preferred grain long-axis directions in the bedding plane. Ns=number of specimens.

Fig. 8. Representative demagnetisation data from: (a,b) the Littleham Mudstone Fm, (c,d) Exmouth Mudstone and Sandstone Fm, (e) Exe Breccia Fm, (f) Dawlish Sandstone Fm, (g) Teignmouth Breccia and (h) Watcombe Fm. a) Specimen L35, normal polarity (behaviour S1, ChRM 500-660^{o}C), b) EM30-4, reverse polarity (behaviour T1, component A, 0-500^{o}C), c) E20, normal polarity (behaviour S2, ChRM 600^{o}C to origin), d) EL63, reverse polarity (behaviour T1, Component A, 0-300^{o}C), e) EB8-1A, normal polarity (behaviour S2, ChRM 300-500^{o}C & 540^{o}C to origin), f) DS21-1, reverse polarity (behaviour T1, steps 500^{o}C and above noisy due to thermal alteration), g) DS4-2, reverse polarity (behaviour S2, ChRM 500-650^{o}C), g) WB1-4, reverse polarity (behaviour S1, ChRM 100-620^{o}C, 680^{o}C step shows thermal alteration). See Figs. 4, 5 for specimen locations.

Fig. 9. a) Stereographic projection of all ChRM directions, with mean of these directions indicated for the units from the Aylesbeare Mudstone Group. B) The progressive unfolding fold test of Watson & Enkin (1993), using the data from the Exeter Group; showing the change in Fisher k with unfolding (left) and a pseudo-sampling bootstrap (right) to estimate the 95% confidence interval on the unfolding %.

Fig. 10. i) Detailed magnetostratigraphic data for the stratigraphic section between the Lympstone sections (3 on Fig. 1) and Littleham Cove. A) Demagnetisation behaviour showing categorisation into good (S1) and poor (S3) ChRM line-fits; great circle fit quality range from good (T1) to poor (T3), and specimens with no Triassic magnetisation are indicated in the P/X column (see text for details). B) Interpreted specimen polarity quality, with those in the greyed column not assigned a polarity. Poorest quality in column headed '??'. C) VGP latitude, with filled symbols for those specimens possessing an S-class ChRM, and unfilled symbols for specimens with T-class, great-circle behaviour. II) Detailed magnetostratigraphic data for the stratigraphic section between Littleham Cove and Budleigh Salterton (1 on Fig. 1). White= reversed polarity, black =normal polarity, grey= uncertain, gap=X. Half bar-width indicates a single useful specimen from this horizon.

Fig. 11. Summary magnetostratigraphic data for European Permian sections, compared to the composite geomagnetic magnetic polarity timescale (GPTS) of Hounslow (submitted). Southern North Sea data for the Leman Sandstone Fm from Turner *et al*. (1999) and Lawton & Robertson (2003). Czaplinek, Piła and Jaworzna IG-1 well data based on Nawrocki (1997) and Słowakiewicz *et al*. (2009). Mirow well from Menning *et al*. (1988) and Langereis *et al*. (2010), Schlierbachswald-4 and Everdingen 1 wells from Szurlies *et al*. (2003), Szurlies (2013). Related Russian stage stratigraphy from Hounslow (submitted). Conodont zones (CZ) labelled with Guadalupian (G) and Lopingian (L) zonal codes from Jin *et al*. (2000) and Shen *et al*. (2010). Early Wuchiapingian carbon isotope excursions (CIE) and Kamura event duration from Chen *et al.* (2011), Isozaki *et al.* (2011).

Type/ Location/ Unit	Dec	Inc	K	α95	Nl/Np	Reversal Test	G_O/G_C	Plat	Plong	Dp/Dm
Littleham Mudstone Fm										
Line fits$	12.4	29.2	26.0	5.4	28/0	R-	11.9/10.4*	53.6	156.3	3.3/6.0
GC means+	10.3	29.2	24.1	4.1	28/25	Rc	11.2/11.2	54.0	159.6	2.5/4.5
Exmouth Mudstone and Sandstone Fm										
Line fits$	14.0	27.1	22.2	4.3	52/0	Rc	11.3/13.3*	52.0	154.2	2.6/4.7
GC means+	14.2	29.0	18.2	3.8	52/27	Rb	2.4/10.0*	53.1	153.5	2.3/4.2
Dawlish Sandstone and Exe Breccia fms										
Line fits$	5.0	26.6	40.4	7.3	11/0	Rc	7.5/20.0	53.2	168.5	4.3/7.9
GC means+	359.4	32.7	8.1	11.3	11/12	Rc	9.6/11.9*	56.9	185.7	7.2/12.8
Teignmouth Breccia Fm										
GC mean+	174.8	-25.1	25.1	8.5	10/3	-	-	52.4	184.8	4.9/9.1
Oddicombe Breccia Fm										
Shaldon and Maidencombe$	191.4	-24.4	116	3.4	16/0	-	-	51.1	158.6	2.0/3.6
Watcombe Fm, basal Oddicombe Breccia										
Watcombe$	173.4	-20.0	28.0	10.7	8/0	-	-	49.5	186.5	5.9/11.2
Knowle Sandstone$	195	-17	6842	3	2/0	-		-	-	-
Exeter Volc. Fm[1]	198	-25	23	6.5	23/0	-		49.5	148.5	-3.8/7.0
Exeter Volc. Fm[2]	189	-19	29	10	9/0	-		48	163	-5.4/10.4
Exeter Grp sediments[2]	188	-14	24	26	3/0	-		-	-	
Aylesbeare Mudstone Grp	13.5	27.8	23.6	3.3	80/0	Rb	6.7/7.4*	52.5	154.9	2.0/3.6
Exeter Grp sediments	3.3	24.8	35.4	3.6	45/0	Rb	5.5/10.0*	52.4	171.2	2.1/3.9

Table 1. Directional means (with tectonic correction), reversal tests and VGP poles. +=great circle combined mean using method of McFadden & McElhinney (1988). $=conventional Fisher mean. Nl=number of specimens using with fitted lines, and Np =number of specimens with great circle planes used in the determining the mean direction. α_{95}, Fisher 95% cone of confidence. k, Fisher precision parameter. G_O is the angular separation between the inverted reverse and normal directions, and Gc is the critical value for the reversal test. In the reversal test the Go/Gc values flagged with * indicate common K values, others not flagged have statistically different K-values for reverse and normal populations, in which case a simulation reversal test was performed. Plat and Plong are the latitude and longitude of the mean virtual geomagnetic pole[1]. From Zijderveld (1967); [2] from Cornwall (1967)

Fig.1

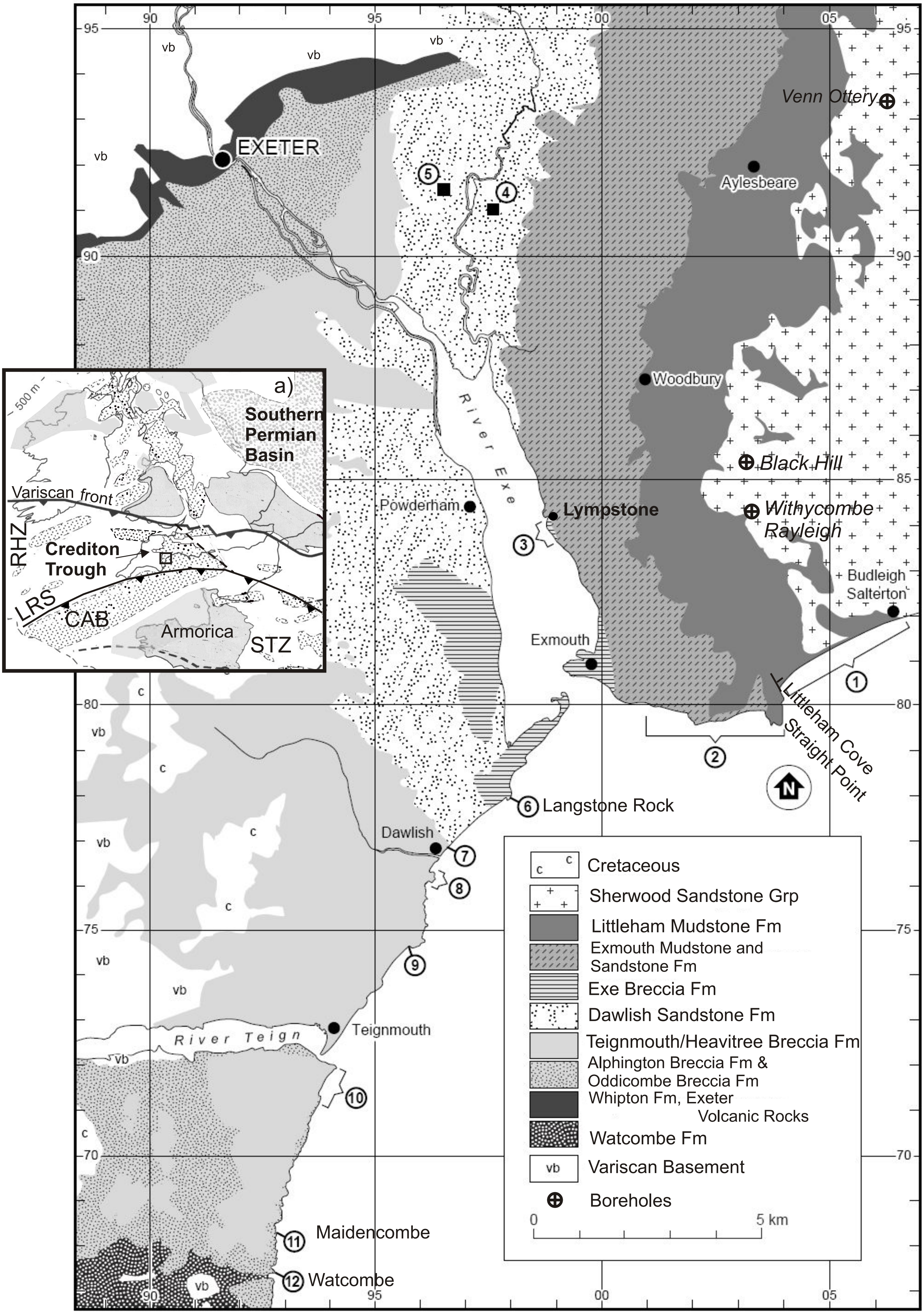

EXETER
vb
Venn Ottery
Aylesbeare
Woodbury
Black Hill
Withycombe Rayleigh
Budleigh Salterton
Lympstone
Powderham
River Exe
Exmouth
Littleham Cove
Straight Point
Langstone Rock
Dawlish
Teignmouth
River Teign
Maidencombe
Watcombe
a)
Southern Permian Basin
Variscan front
RHZ
Crediton Trough
LRS
CAB
Armorica
STZ
500 m
Cretaceous
Sherwood Sandstone Grp
Littleham Mudstone Fm
Exmouth Mudstone and Sandstone Fm
Exe Breccia Fm
Dawlish Sandstone Fm
Teignmouth/Heavitree Breccia Fm
Alphington Breccia Fm & Oddicombe Breccia Fm
Whipton Fm, Exeter Volcanic Rocks
Watcombe Fm
Variscan Basement
Boreholes
0
5 km
N

Fig.2

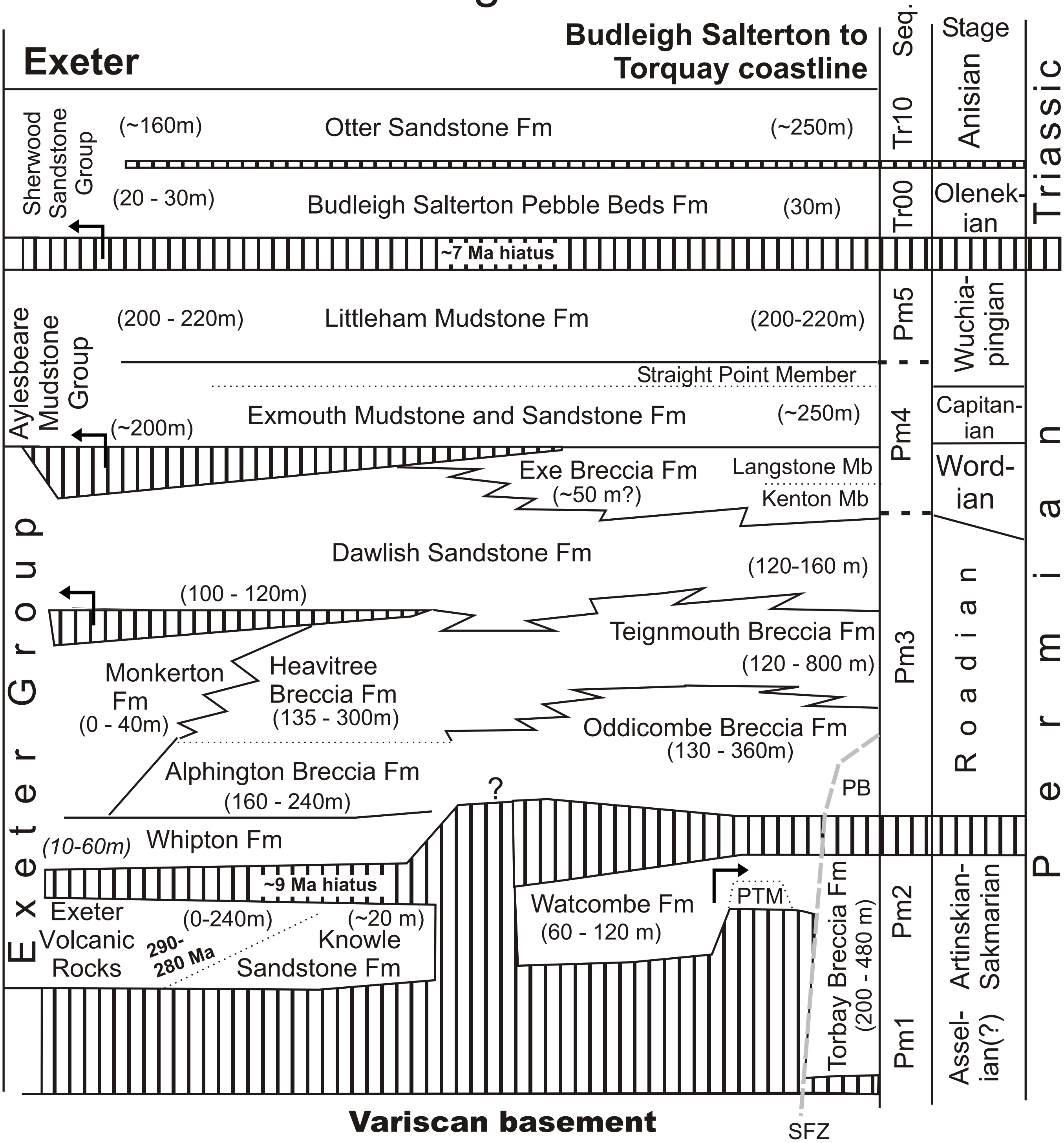
Exeter
Budleigh Salterton to Torquay coastline
Seq.
Stage
Triassic
Permian
Sherwood Sandstone Group
(~160m)
Otter Sandstone Fm
(~250m)
Tr10
Anisian
(20 - 30m)
Budleigh Salterton Pebble Beds Fm
(30m)
Tr00
Olenek-ian
~7 Ma hiatus
Aylesbeare Mudstone Group
(200 - 220m)
Littleham Mudstone Fm
(200-220m)
Pm5
Wuchia-pingian
Straight Point Member
Exmouth Mudstone and Sandstone Fm
(~200m)
(~250m)
Pm4
Capitan-ian
Exe Breccia Fm
(~50 m?)
Langstone Mb
Kenton Mb
Word-ian
Exeter Group
Dawlish Sandstone Fm
(120-160 m)
(100 - 120m)
Teignmouth Breccia Fm
(120 - 800 m)
Roadian
Pm3
Monkerton Fm
(0 - 40m)
Heavitree Breccia Fm
(135 - 300m)
Oddicombe Breccia Fm
(130 - 360m)
Alphington Breccia Fm
(160 - 240m)
?
PB
(10-60m)
Whipton Fm
~9 Ma hiatus
Exeter Volcanic Rocks
(0-240m)
290-280 Ma
(~20 m)
Knowle Sandstone Fm
Watcombe Fm
(60 - 120 m)
PTM
Torbay Breccia Fm
(200 - 480 m)
Pm2
Artinskian-Sakmarian
Pm1
Assel-ian(?)
Variscan basement
SFZ

Fig.3

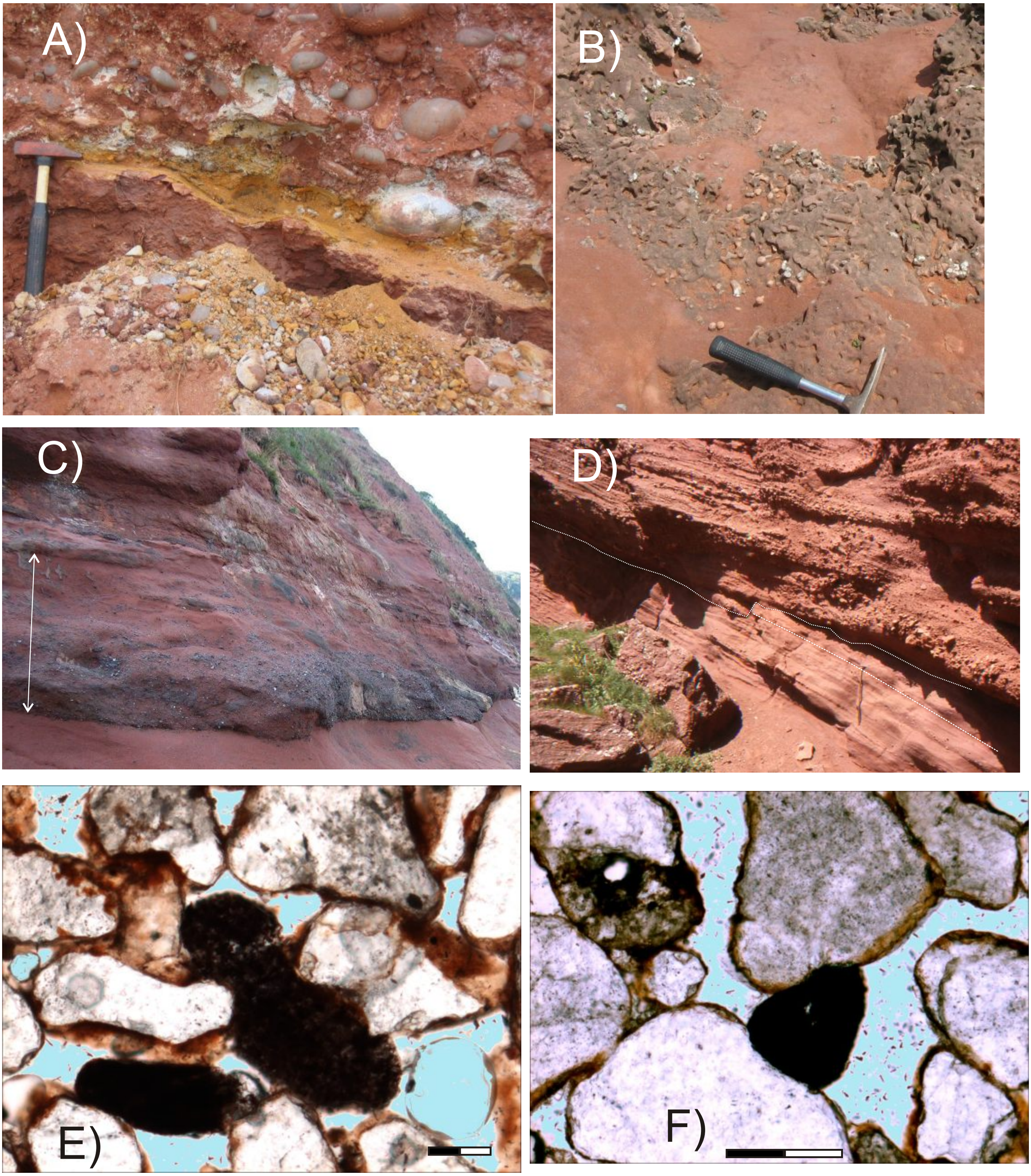

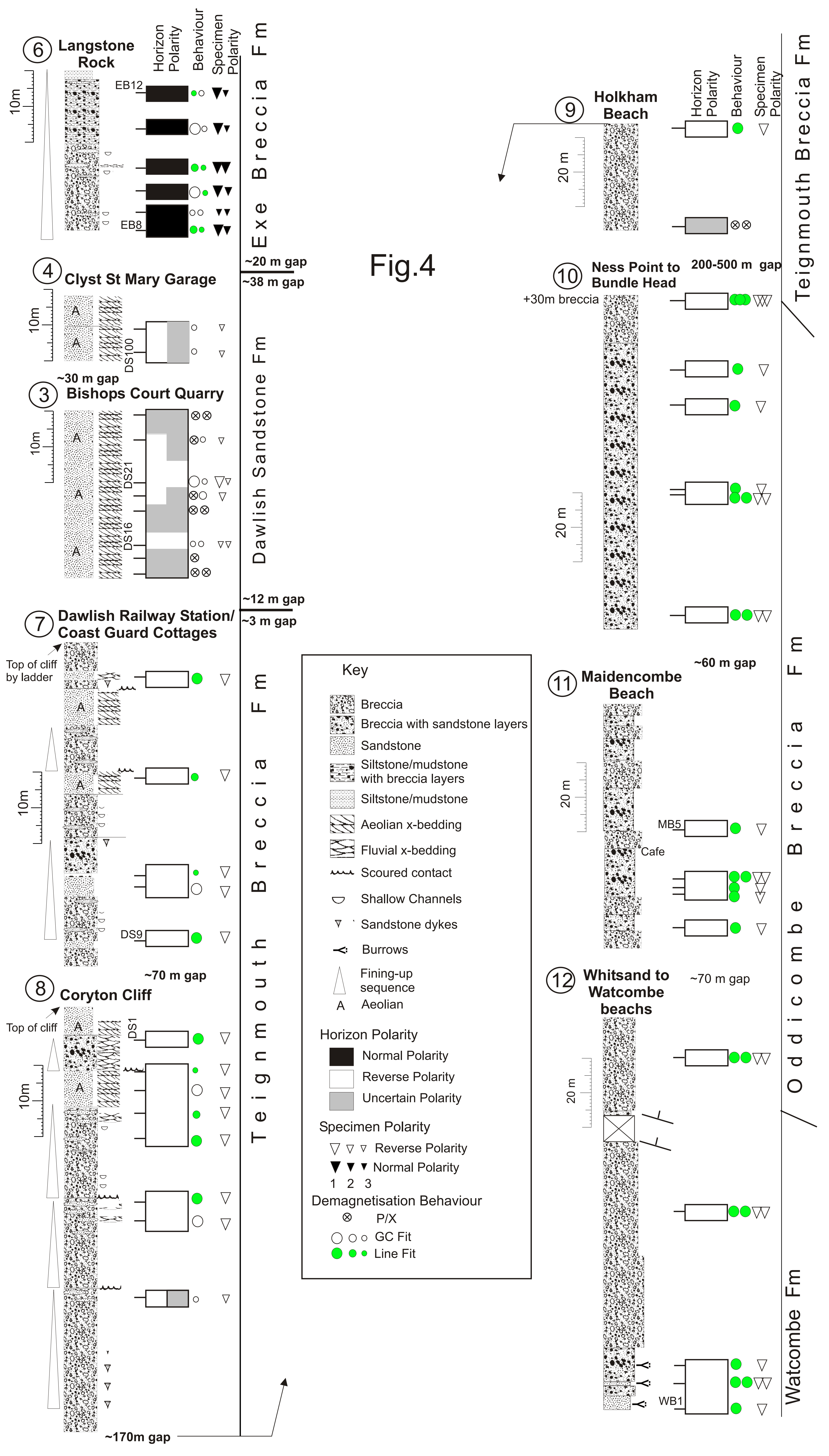

Fig.4
6 Langstone Rock
Horizon Polarity
Behaviour
Specimen Polarity
EB12
EB8
10m
Exe Breccia Fm
~20 m gap
~38 m gap
4 Clyst St Mary Garage
A
DS100
~30 m gap
3 Bishops Court Quarry
DS21
DS16
Dawlish Sandstone Fm
~12 m gap
~3 m gap
7 Dawlish Railway Station/ Coast Guard Cottages
Top of cliff by ladder
DS9
~70 m gap
8 Coryton Cliff
Top of cliff
DS1
~170m gap
Teignmouth Breccia Fm
9 Holkham Beach
20 m
10 Ness Point to Bundle Head
200-500 m gap
+30m breccia
~60 m gap
11 Maidencombe Beach
MB5
Cafe
12 Whitsand to Watcombe beachs
~70 m gap
WB1
Oddicombe Breccia Fm
Watcombe Fm
Key
Breccia
Breccia with sandstone layers
Sandstone
Siltstone/mudstone with breccia layers
Siltstone/mudstone
Aeolian x-bedding
Fluvial x-bedding
Scoured contact
Shallow Channels
Sandstone dykes
Burrows
Fining-up sequence
A Aeolian
Horizon Polarity
Normal Polarity
Reverse Polarity
Uncertain Polarity
Specimen Polarity
Reverse Polarity
Normal Polarity
1 2 3
Demagnetisation Behaviour
P/X
GC Fit
Line Fit

Fig.5

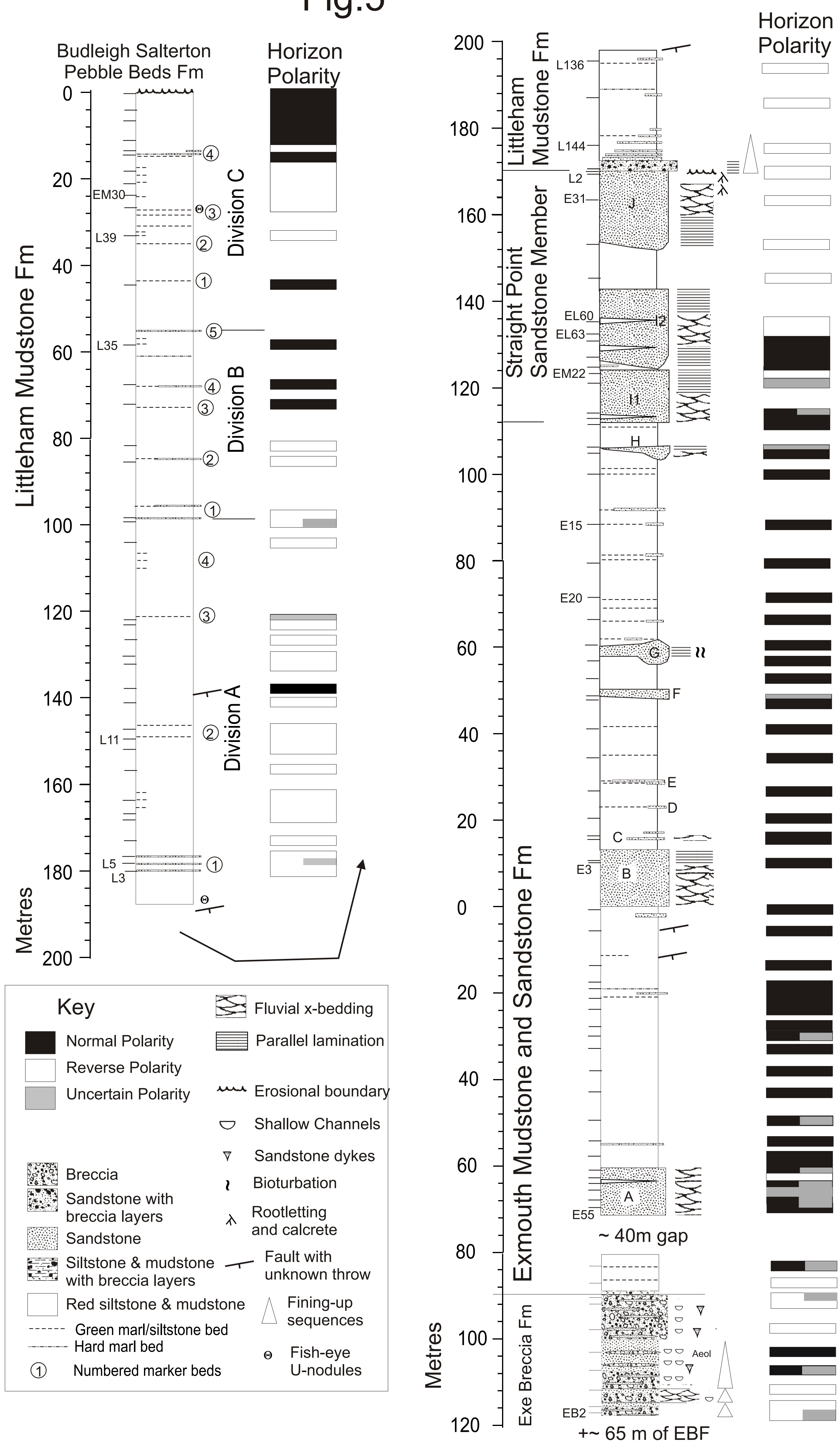

Budleigh Salterton Pebble Beds Fm
Horizon Polarity
Littleham Mudstone Fm
Division C
Division B
Division A
EM30
L39
L35
L11
L5
L3
Metres
Key
Normal Polarity
Reverse Polarity
Uncertain Polarity
Breccia
Sandstone with breccia layers
Sandstone
Siltstone & mudstone with breccia layers
Red siltstone & mudstone
Green marl/siltstone bed
Hard marl bed
Numbered marker beds
Fluvial x-bedding
Parallel lamination
Erosional boundary
Shallow Channels
Sandstone dykes
Bioturbation
Rootletting and calcrete
Fault with unknown throw
Fining-up sequences
Fish-eye U-nodules
Littleham Mudstone Fm
Straight Point Sandstone Member
Exmouth Mudstone and Sandstone Fm
Exe Breccia Fm
L136
L144
L2
E31
EL60
EL63
EM22
E15
E20
E3
E55
EB2
~ 40m gap
+~ 65 m of EBF
Aeol
Horizon Polarity
Metres

Fig.6

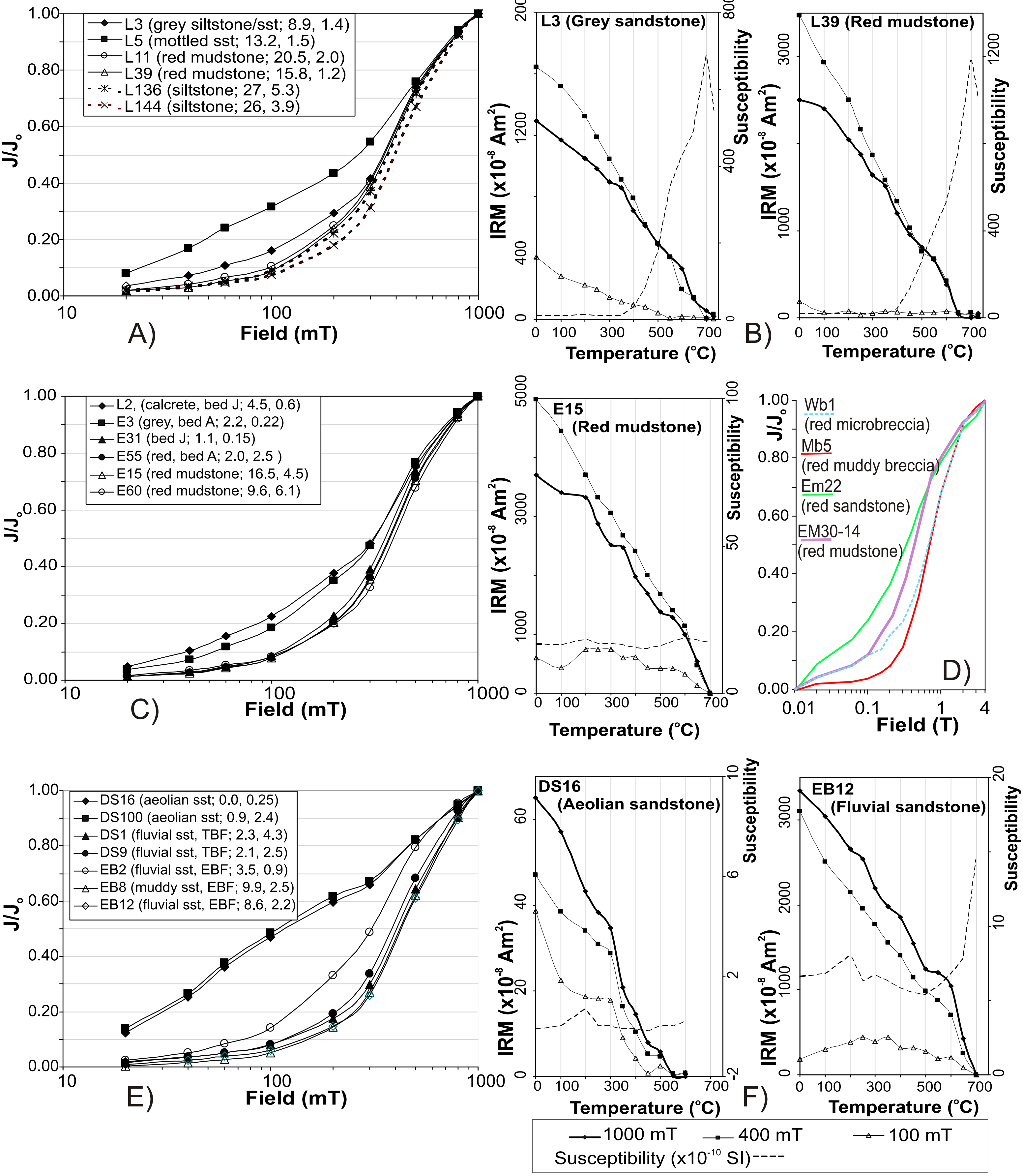
L3 (grey siltstone/sst; 8.9, 1.4)
L5 (mottled sst; 13.2, 1.5)
L11 (red mudstone; 20.5, 2.0)
L39 (red mudstone; 15.8, 1.2)
L136 (siltstone; 27, 5.3)
L144 (siltstone; 26, 3.9)
J/J$_o$
Field (mT)
A)
L3 (Grey sandstone)
L39 (Red mudstone)
IRM (x10^{-8} Am^2)
Susceptibility
Temperature (°C)
B)
L2, (calcrete, bed J; 4.5, 0.6)
E3 (grey, bed A; 2.2, 0.22)
E31 (bed J; 1.1, 0.15)
E55 (red, bed A; 2.0, 2.5)
E15 (red mudstone; 16.5, 4.5)
E60 (red mudstone; 9.6, 6.1)
C)
E15 (Red mudstone)
Wb1 (red microbreccia)
Mb5 (red muddy breccia)
Em22 (red sandstone)
EM30-14 (red mudstone)
Field (T)
D)
DS16 (aeolian sst; 0.0, 0.25)
DS100 (aeolian sst; 0.9, 2.4)
DS1 (fluvial sst, TBF; 2.3, 4.3)
DS9 (fluvial sst, TBF; 2.1, 2.5)
EB2 (fluvial sst, EBF; 3.5, 0.9)
EB8 (muddy sst, EBF; 9.9, 2.5)
EB12 (fluvial sst, EBF; 8.6, 2.2)
E)
DS16 (Aeolian sandstone)
EB12 (Fluvial sandstone)
F)
1000 mT
400 mT
100 mT
Susceptibility (x10^{-10} SI)----

Fig.7

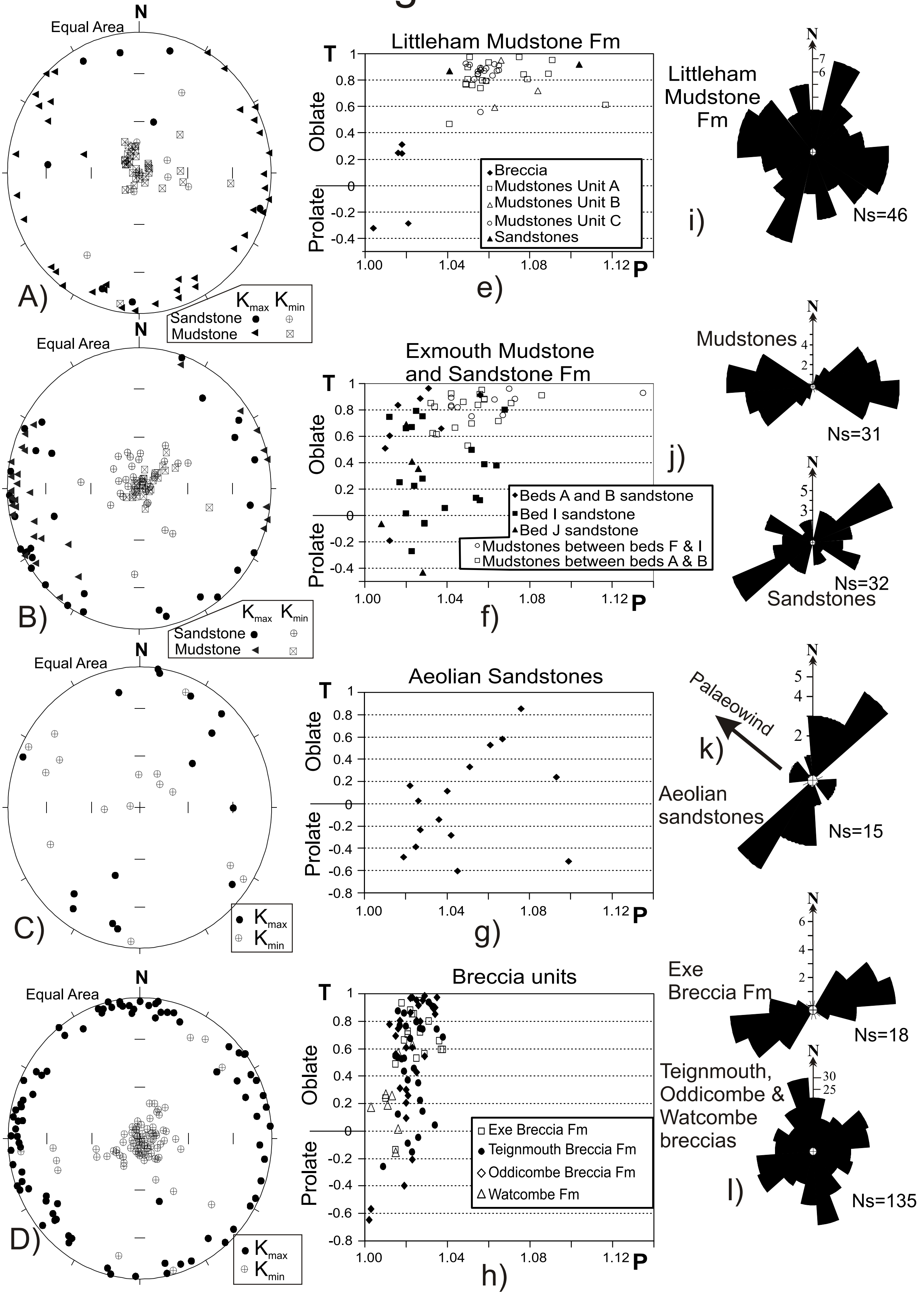

A)
Equal Area
N
K_{max} K_{min}
Sandstone
Mudstone
Littleham Mudstone Fm
T
Oblate
Prolate
Breccia
Mudstones Unit A
Mudstones Unit B
Mudstones Unit C
Sandstones
1.00 1.04 1.08 1.12 P
e)
Littleham Mudstone Fm
i)
Ns=46
B)
Equal Area
N
K_{max} K_{min}
Sandstone
Mudstone
Exmouth Mudstone and Sandstone Fm
T
Oblate
Prolate
Beds A and B sandstone
Bed I sandstone
Bed J sandstone
Mudstones between beds F & I
Mudstones between beds A & B
1.00 1.04 1.08 1.12 P
f)
Mudstones
Ns=31
j)
Ns=32
Sandstones
C)
Equal Area
N
K_{max}
K_{min}
Aeolian Sandstones
T
Oblate
Prolate
1.00 1.04 1.08 1.12 P
g)
Palaeowind
k)
Aeolian sandstones
Ns=15
D)
Equal Area
N
K_{max}
K_{min}
Breccia units
T
Oblate
Prolate
Exe Breccia Fm
Teignmouth Breccia Fm
Oddicombe Breccia Fm
Watcombe Fm
1.00 1.04 1.08 1.12 P
h)
Exe Breccia Fm
Ns=18
Teignmouth, Oddicombe & Watcombe breccias
l)
Ns=135

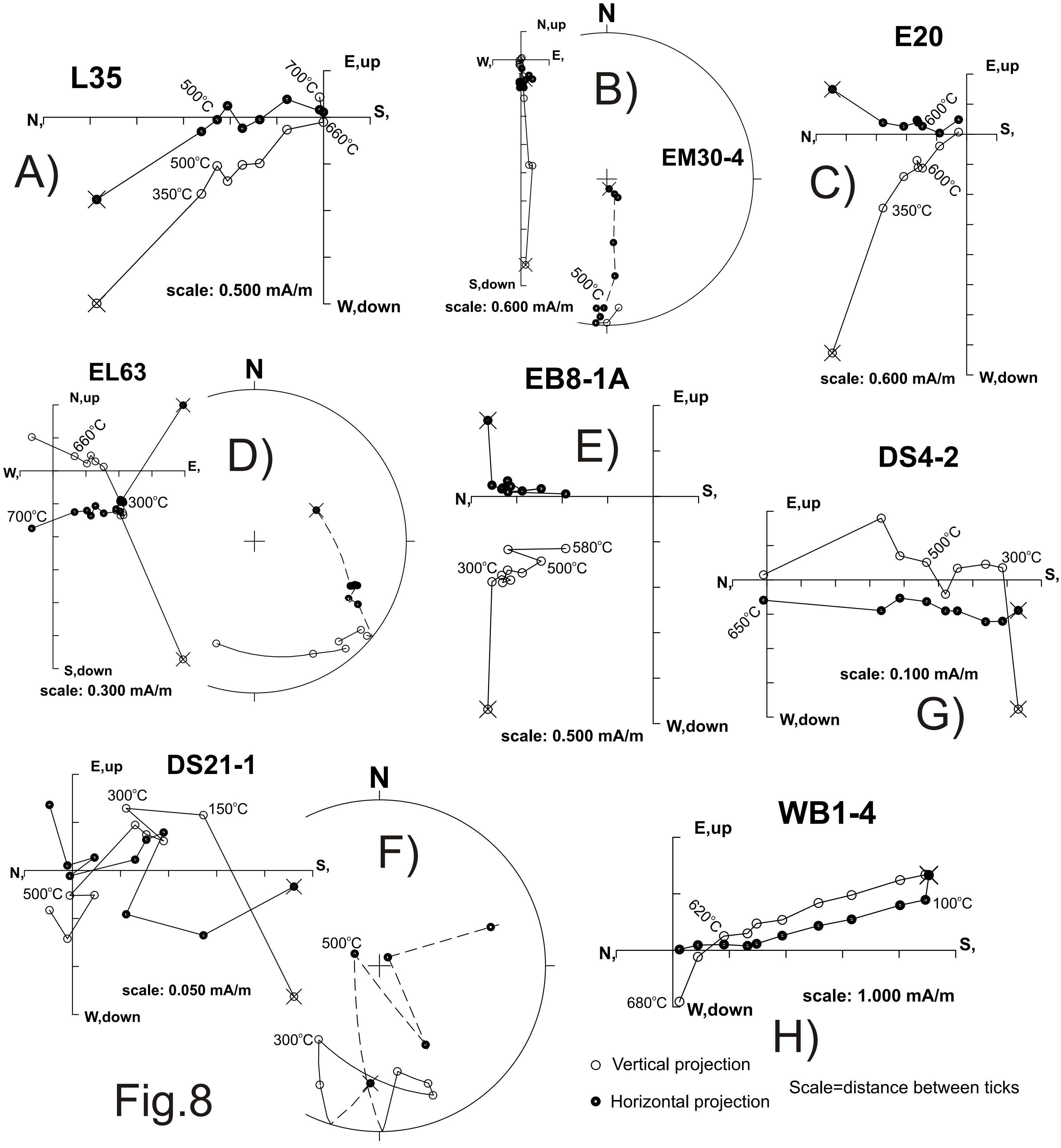
L35
A)
E,up
N,
S,
W,down
700°C
500°C
660°C
500°C
350°C
scale: 0.500 mA/m
B)
EM30-4
N
N,up
W,
E,
S,down
500°C
scale: 0.600 mA/m
E20
C)
E,up
N,
S,
W,down
600°C
600°C
350°C
scale: 0.600 mA/m
EL63
D)
N
N,up
W,
E,
S,down
660°C
700°C
300°C
scale: 0.300 mA/m
EB8-1A
E)
E,up
N,
S,
W,down
580°C
300°C
500°C
scale: 0.500 mA/m
DS4-2
G)
E,up
N,
S,
W,down
500°C
300°C
650°C
scale: 0.100 mA/m
DS21-1
F)
N
E,up
N,
S,
W,down
300°C
150°C
500°C
500°C
300°C
scale: 0.050 mA/m
WB1-4
H)
E,up
N,
S,
W,down
620°C
100°C
680°C
scale: 1.000 mA/m
Vertical projection
Horizontal projection
Scale=distance between ticks

Fig.8

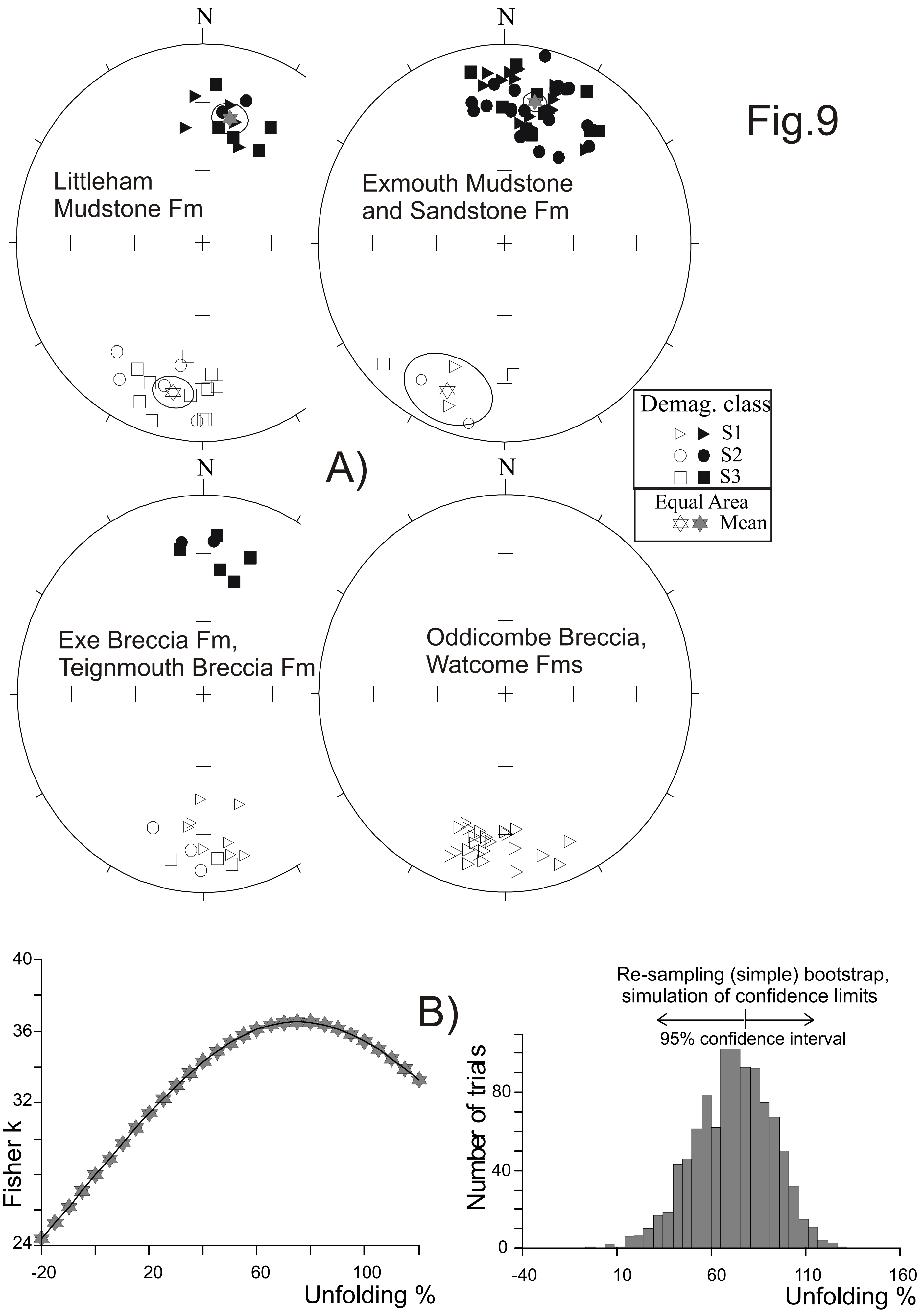
Fig.9
N
Littleham Mudstone Fm
Exmouth Mudstone and Sandstone Fm
A)
Exe Breccia Fm, Teignmouth Breccia Fm
Oddicombe Breccia, Watcome Fms
Demag. class
S1
S2
S3
Equal Area
Mean
B)
Fisher k
Unfolding %
Re-sampling (simple) bootstrap, simulation of confidence limits
95% confidence interval
Number of trials
Unfolding %

Fig.10a

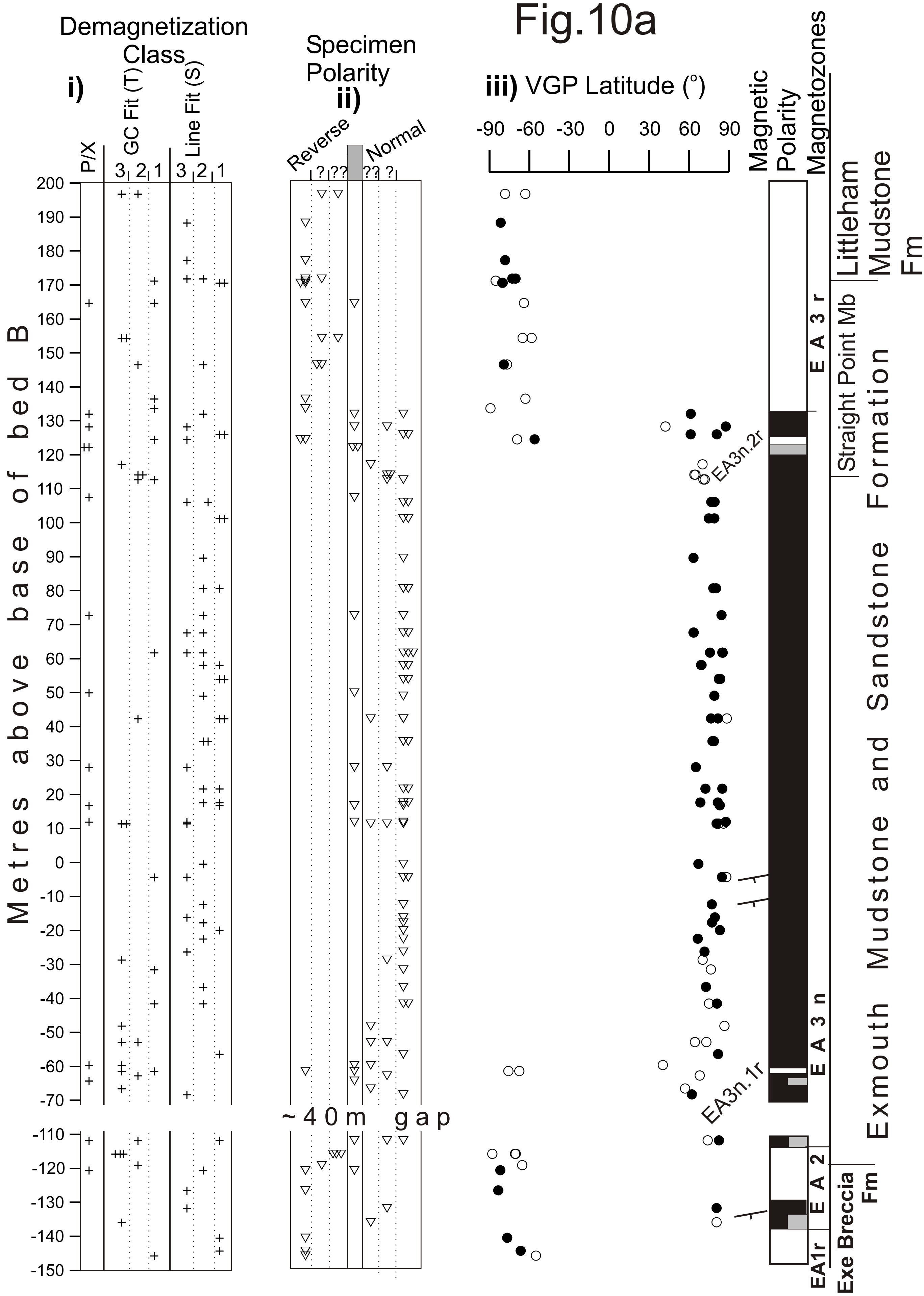

Demagnetization Class
i)
P/X
GC Fit (T)
Line Fit (S)
3 2 1
Specimen Polarity
ii)
Reverse
Normal
? ??
?? ?
iii) VGP Latitude (°)
-90 -60 -30 0 30 60 90
Magnetic Polarity
Magnetozones
Metres above base of bed B
~40m gap
EA3n.2r
EA3n.1r
E A 3 r
E A 3 n
E A 2
EA1r
Littleham Mudstone Fm
Straight Point Mb
Exmouth Mudstone and Sandstone Formation
Exe Breccia Fm

Fig.10b

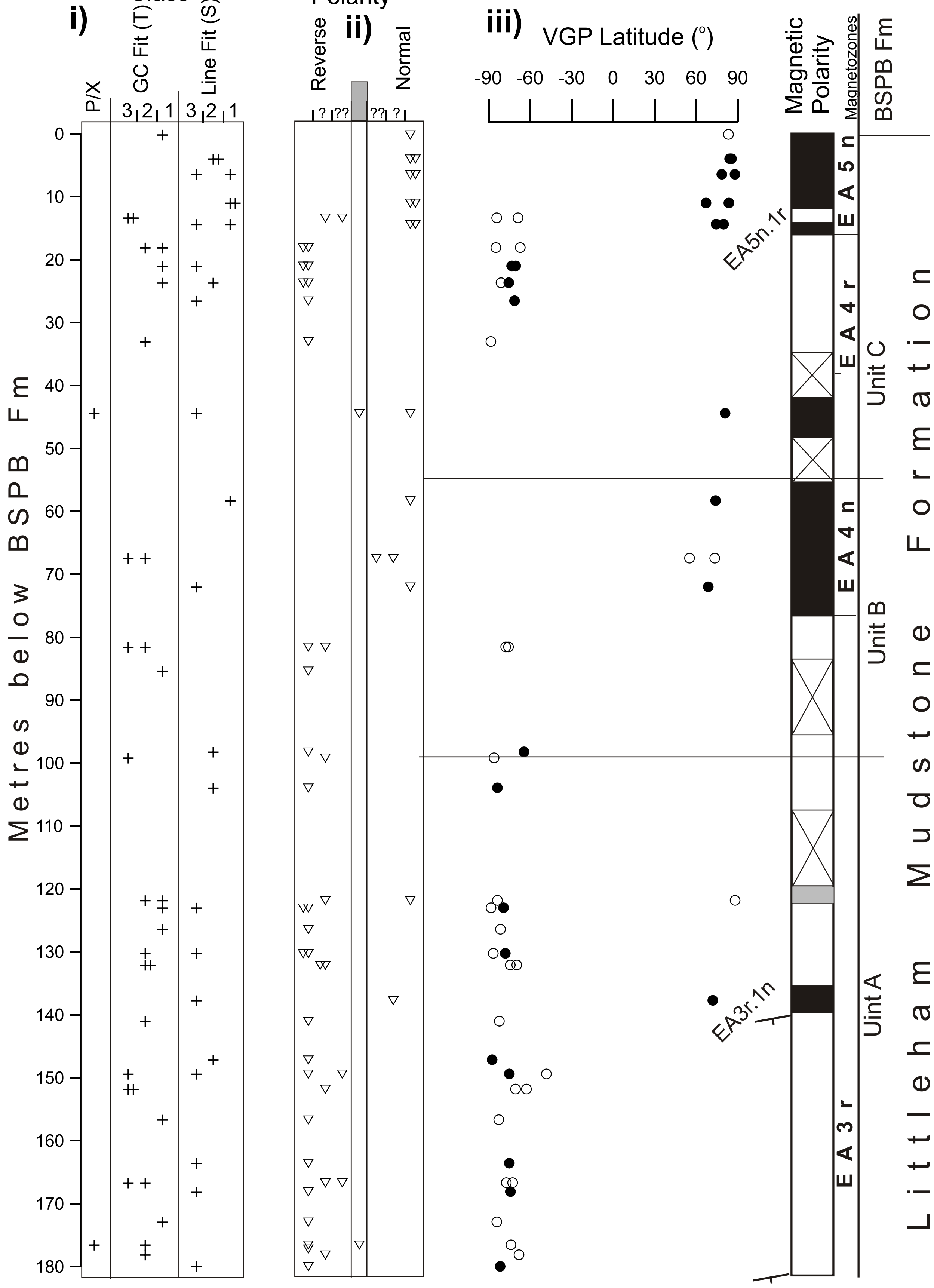

Demagnetization Class
i)
P/X
GC Fit (T)
Line Fit (S)
3 2 1 3 2 1
Specimen Polarity
ii)
Reverse
Normal
? ?? ?? ?
iii)
VGP Latitude (°)
-90 -60 -30 0 30 60 90
Magnetic Polarity
Magnetozones
BSPB Fm
Metres below BSPB Fm
0
10
20
30
40
50
60
70
80
90
100
110
120
130
140
150
160
170
180
E A 5 n
EA5n.1r
E A 4 r
E A 4 n
EA3r.1n
E A 3 r
Unit C
Unit B
Uint A
Littleham Mudstone Formation

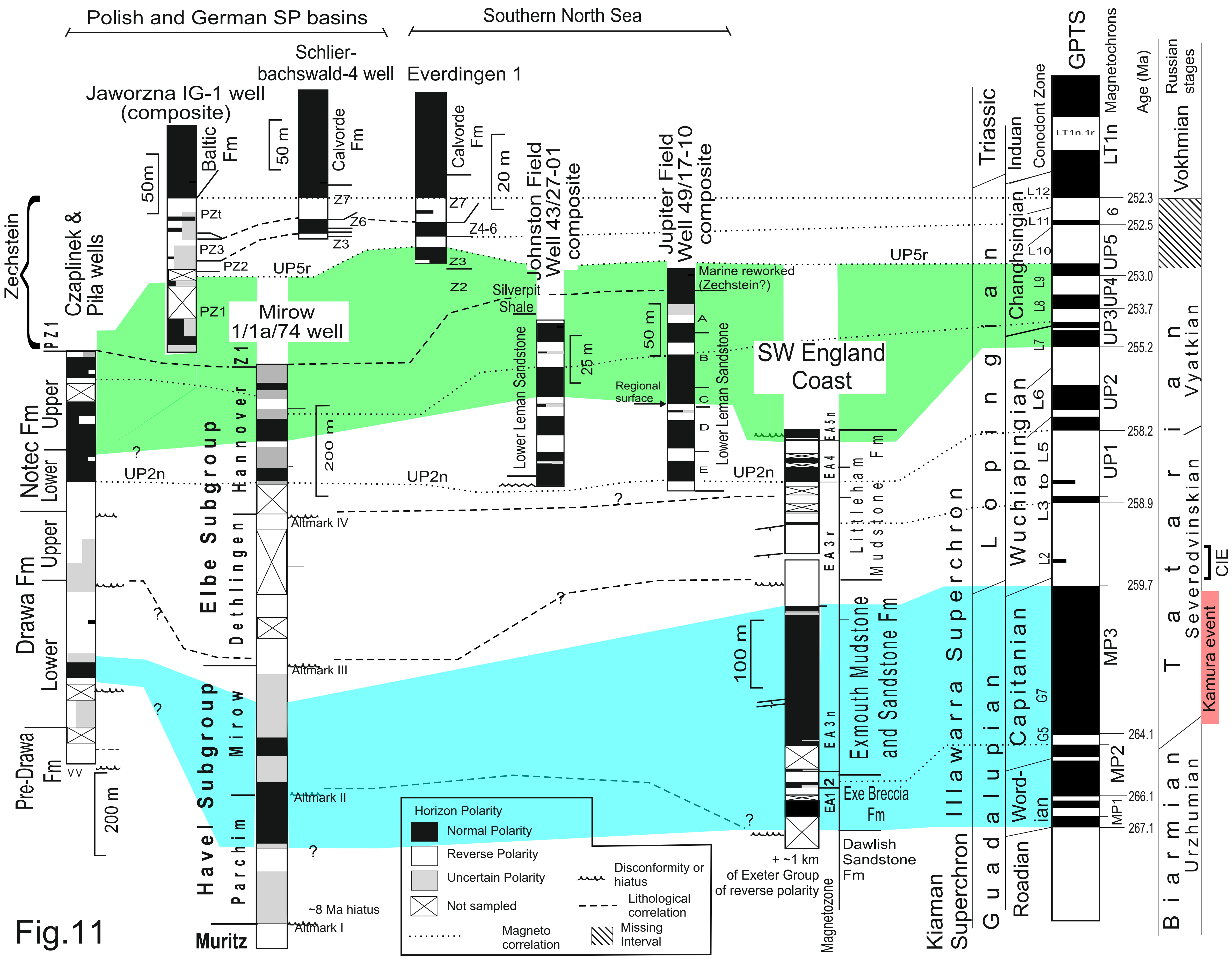
Polish and German SP basins
Southern North Sea
Jaworzna IG-1 well (composite)
Schlier-bachswald-4 well
Everdingen 1
Johnston Field Well 43/27-01 composite
Jupiter Field Well 49/17-10 composite
Czaplinek & Piła wells
Mirow 1/1a/74 well
SW England Coast
Zechstein
Baltic Fm
Calvorde Fm
50m
50 m
20 m
25 m
200 m
100 m
PZt
PZ3
PZ2
PZ1
Z7
Z6
Z4-6
Z3
Z2
Z1
UP5r
UP2n
Silverpit Shale
Marine reworked (Zechstein?)
Regional surface
Lower Leman Sandstone
Notec Fm
Upper
Lower
Drawa Fm
Pre-Drawa Fm
Elbe Subgroup
Havel Subgroup
Hannover
Dethlingen
Mirow
Parchim
Muritz
Altmark IV
Altmark III
Altmark II
Altmark I
~8 Ma hiatus
Littleham Mudstone Fm
Exmouth Mudstone and Sandstone Fm
Exe Breccia Fm
Dawlish Sandstone Fm
+ ~1 km of Exeter Group of reverse polarity
EA5n
EA4
EA3r
EA3n
EA2
EA1
Magnetozone
Horizon Polarity
Normal Polarity
Reverse Polarity
Uncertain Polarity
Not sampled
Disconformity or hiatus
Lithological correlation
Magneto correlation
Missing Interval
Kiaman Superchron
Illawarra Superchron
Triassic
Lopingian
Guadalupian
Induan
Changhsingian
Wuchiapingian
Capitanian
Wordian
Roadian
Conodont Zone
L12
L11
L10
L9
L8
L7
L6
L3 to L5
L2
G7
G5
GPTS
Magnetochrons
LT1n.1r
LT1n
6
UP5
UP4
UP3
UP2
UP1
MP3
MP2
MP1
Age (Ma)
252.3
252.5
253.0
253.7
255.2
258.2
258.9
259.7
264.1
266.1
267.1
Russian stages
Vokhmian
Tatarian
Vyatkian
Severodvinskian
Biarmian
Urzhumian
CIE
Kamura event

Fig.11